Drift Chamber in IDEA as an alternative concept

Nicola De Filippis

Politecnico and INFN Bari

2025 International Workshop on the
High Energy Circular Electron Positron Collider (CEPC2025)
Guangzhou, November 6-10, 2025

The IDEA detector at e^+e^- colliders

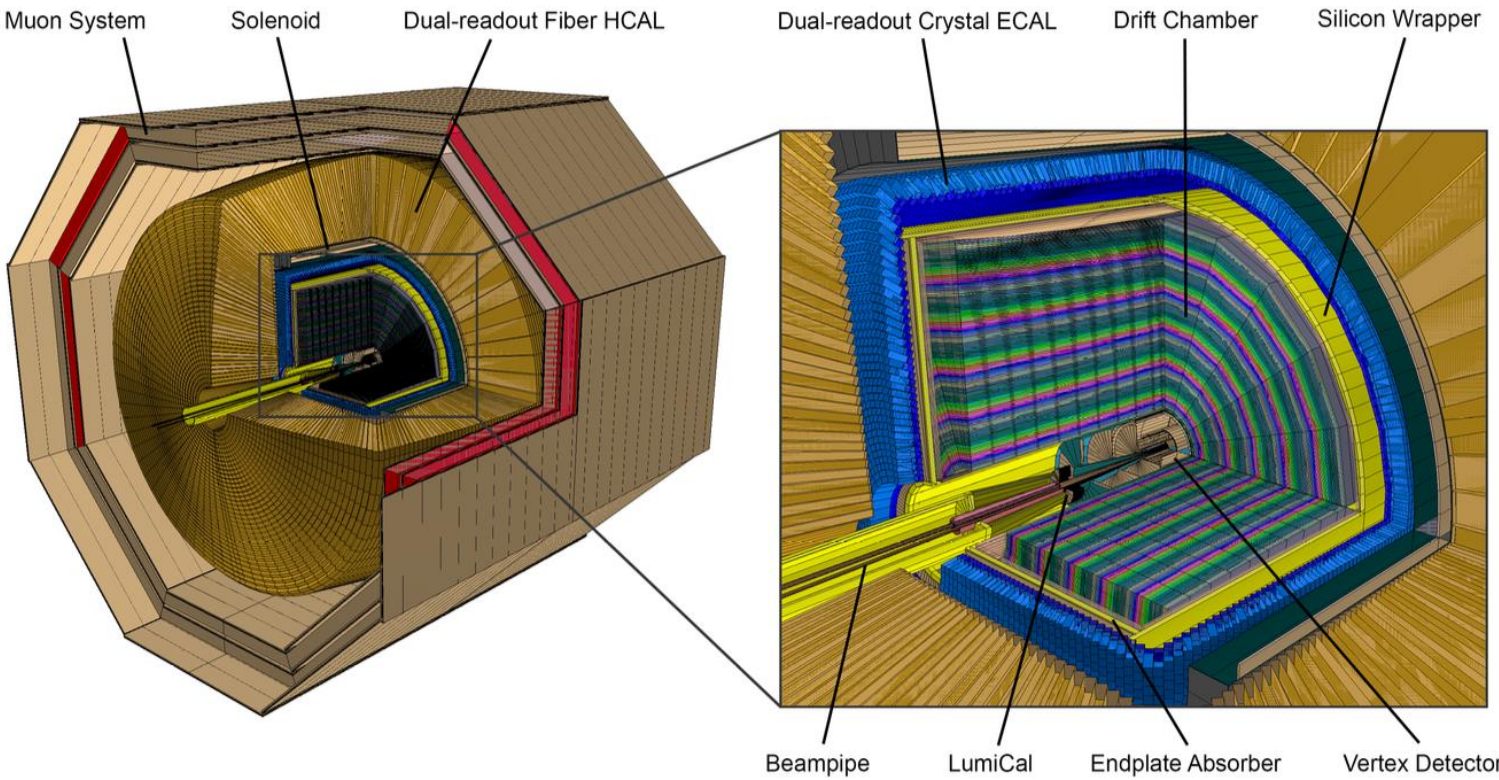

IDEA (**Innovative Detector for E+e- Accelerato)** consists of:

- a silicon pixel vertex detector
- a large-volume extremely-light **drift chamber**
- surrounded by a layer of silicon micro-strip detectors
- a thin low-mass superconducting solenoid coil
- a preshower detector based on **μ-WELL technology**
- a dual read-out calorimeter
- muon chambers inside the magnet return yoke, based on **μ-WELL technology**

arXiv:2502.21223v4

The IDEA Drift Chamber: evolution and new concepts

KLOE (1998) → **CMD-2** (2006) → **MEG2** (2014) → **IDEA** (2017)

- New mechanical assembly procedure by separating the gas containment from the wire support functions
- New concepts for wire tension compensation resulting in end caps with a 5% X_0 (including front end electronics and cables) and 1.6% X_0 in the radial direction
- A larger number of thinner and lighter wires resulting in less total stress on end plates
- No use of massive feed-through → Feed-through-less wiring
- Use of cluster counting for particle identification
- Use of cluster timing for improving spatial resolution

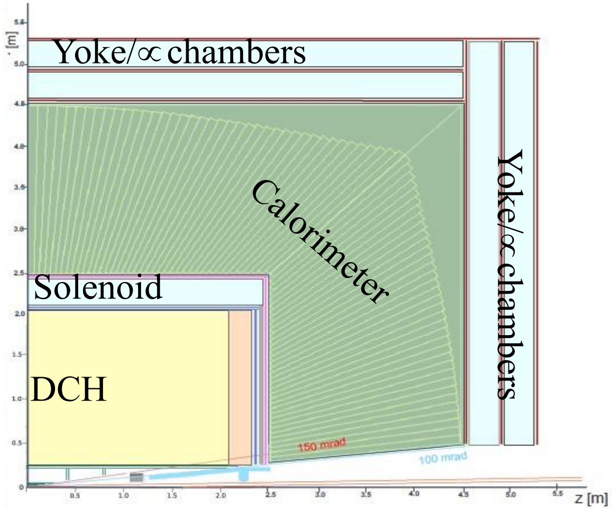

The Drift Chamber of IDEA

The DCH is:

- a unique-volume, high granularity, fully stereo, low-mass cylindrical
- gas: He 90% - iC_4H_{10} 10%
- inner radius R_{in} = 0.35m, outer radius R_{out} = 2m
- length L = 4m
- drift length ~1 cm
- drift time up to 400ns
- σ_{xy} < 100 μm, σ_z < 1 mm
- 12÷14.5 mm wide square cells, 5 : 1 field to sense wires ratio
- 112 co-axial layers (grouped in 14 superlayers of 8 layers), at alternating-sign stereo angles, in 24 azimuthal sectors
- 343968 wires in total:

  sense vires: 20 μm diameter W(Au) = > 56448 wires

  field wires: 40 μm diameter Al(Ag) = > 229056 wires

  f. and g. wires: 50 μm diameter Al(Ag) = > 58464 wires

- the wire net created by the combination of + and – orientation generates a more uniform equipotential surface → better E-field isotropy and smaller ExB asymmetries)

- thin wires → increase the chamber granularity → reducing both multiple scattering and the overall tension on the endplates

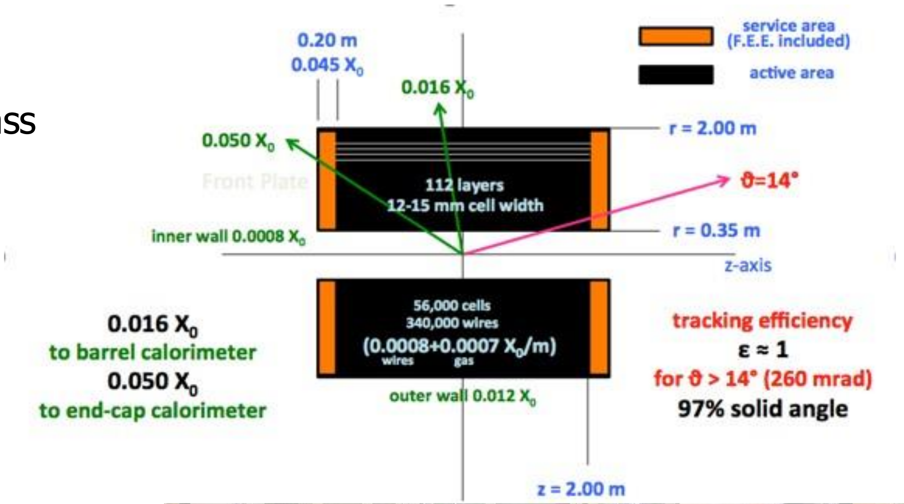

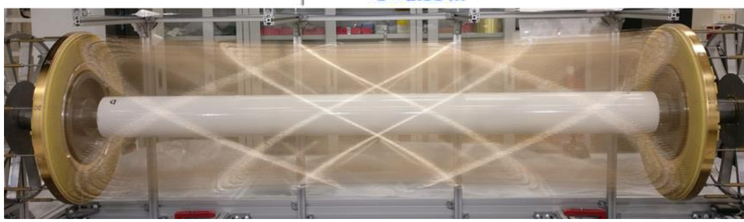

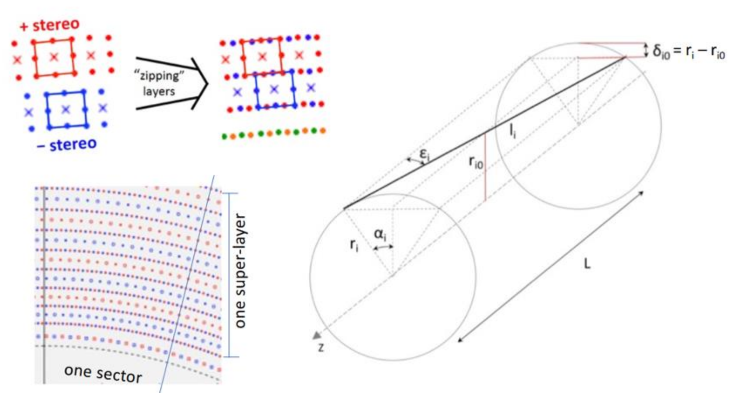

Stereo configuration: one sector is connected with the second corresponding sector in the opposite endcap (hyperbolic profile).

Challenges: wire studies

Wire constraints

Electrostatic stability condition

$$T_c \geq \frac{C^2 V_0^2}{4\pi\epsilon w^2} L^2$$

T_c wire tension
w cell width
L wire length

C capacitance per unit length
V_0 voltage anode-cathode

For w = 1 cm, L = 4 m:

T_c > 26 g for 40 µm Al field wires (δ_{grav} = 260 μm)
T_c > 21 g for 20 µm W sense wires (δ_{grav} = 580 μm)

Elastic limit condition

$$T_c < YTS \times \pi \cdot r_w^2$$

YTS = 750 Mpa for W, *290 Mpa for Al*

T_c < 36 g for 40 µm Al field wires (δ_{grav} = 190 μm)
T_c < 24 g for 20 µm W sense wires (δ_{grav} = 510 μm)

The drift chamber length (**L = 4 m**) imposes strong constraints on the drift cell size (**w = 1 cm**)
Very little margin left ⇒ increase wires radii or cell size
⇒ use different types of wires

The proposed drift chambers for FCC-ee and CEPC have lengths **L = 4 m** and plan to exploit the cluster counting technique, which requires gas gains **~5×10^5**.
This poses serious constraints on the drift cell width (**w**) and on the wire material (**YTS**).

⇒ new wire material studies

Wire tests with standard protocol

Tests started in a clean room at INFN Bari:

- 20 μm diameter tungsten wire coated with gold
- 20 μm diameter molibdenum coated with gold
- 33.5 μm diameter carbon monofilament
- aluminium field wires to be tested

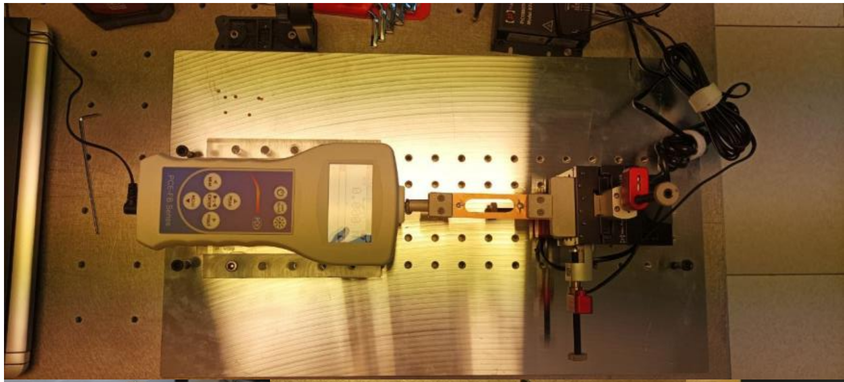

Setup:

- 3 axis picometer slides (30nm step)
- digital dynamometer (acc. 0.001N)

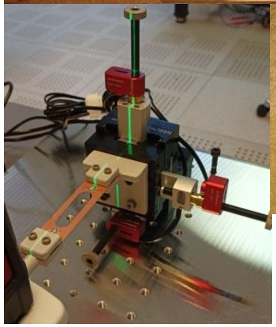

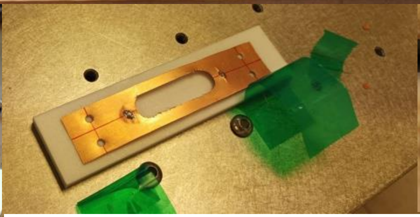

Protocol for measurements:

- **Scope**: Tensile Strength and Young's modulus for High-Modulus (>21 GPa) Single-Filament Materials (gage length > 2000*wire diameter)
- **Summary**: the filaments are center-line mounted on special slotted tabs. The tabs are gripped so that the test specimen is aligned axially in the jaws of a constant-speed movable-crosshead test machine. The filaments are then stressed to failure at a constant strain rate.

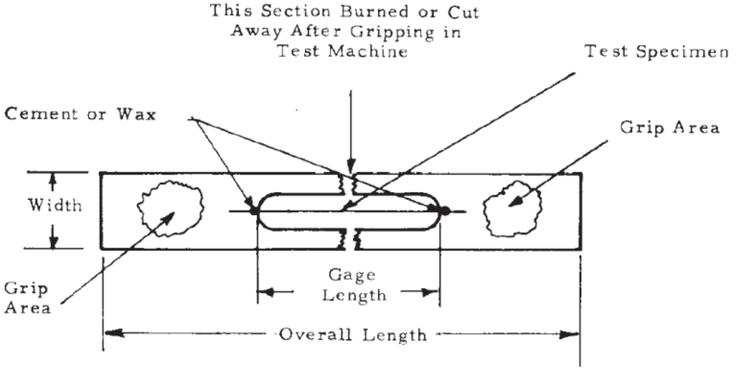

Gold-plated tungsten wire

- W with Z=74
- 20 μm diameter wire
- conductive and easy to solder

Specimen number	Tensile Strength - UTS (GPa)	Young module (Gpa)	R^2	Effective test time (s)	Total wire elongation (mm)	Elongation (%)	Fracture strain - ε_f (%)	Elongation at break (%)	Elastic limit strain - ε_y(%)	Yield Tensile Strength - YTS (GPa)
1	2.811	186.561	0.9990	34.15	2.049	4.098	0.041	4.098	0.009	1.673
2	2.820	172.631	0.9980	35.23	2.114	4.227	0.042	4.227	0.009	1.548
3	2.814	178.624	0.9995	38.90	2.334	4.668	0.048	4.800	0.008	1.334
4	2.718	172.790	0.9998	40.00	2.400	4.800	0.048	4.800	0.009	1.550
5	2.833	185.590	0.9993	34.88	2.093	4.185	0.042	4.185	0.009	1.665
Av. Set	2.799	179.239	0.9991	36.63	2.198	4.396	0.044	4.422	0.009	1.554
11	2.843	211.047	0.9972	33.70	2.022	4.044	0.040	4.044	0.009	1.893
33	2.827	220.920	0.9991	29.30	1.758	3.516	0.035	3.516	0.009	1.982
34	2.839	246.097	0.9962	26.48	1.589	3.177	0.032	3.177	0.009	2.207
35	2.820	246.673	0.9974	25.13	1.508	3.015	0.030	3.015	0.009	2.213
36	2.820	209.416	0.9998	29.13	1.748	3.495	0.035	3.495	0.009	1.878
Av. Set	2.830	226.831	0.9980	28.75	1.725	3.449	0.034	3.449	0.009	2.035
12	2.817	295.044	0.9998	45.58	1.367	2.735	0.027	2.735	0.006	1.766
13	2.811	289.015	0.9992	40.53	1.216	2.432	0.024	2.432	0.006	1.730
15	2.820	278.925	0.9997	47.95	1.439	2.877	0.029	2.877	0.006	1.669
16	2.814	303.444	0.9997	43.55	1.307	2.613	0.026	2.613	0.005	1.361
37	2.843	308.218	0.9998	41.90	1.257	2.514	0.027	2.735	0.004	1.382
Av. Set	2.821	294.929	0.9996	43.90	1.317	2.634	0.027	2.678	0.005	1.582
17	2.807	281.131	0.9998	64.75	1.295	2.590	0.026	2.590	0.006	1.684
18	2.811	283.814	0.9997	62.95	1.259	2.518	0.025	2.517	0.006	1.700
19	2.792	274.393	0.9997	64.15	1.283	2.566	0.026	2.566	0.006	1.644
20	2.792	282.702	0.9996	64.75	1.295	2.590	0.026	2.590	0.006	1.693
38	2.792	291.537	0.9997	60.63	1.213	2.425	0.024	2.425	0.006	1.746
Av. Set	2.799	282.715	0.9997	63.45	1.269	2.538	0.025	2.538	0.006	1.693

v=60 μm/s
l=60mm

v=60 μm/s
l=50mm

v=30 μm/s
l=50mm

v=20 μm/s
l=50mm

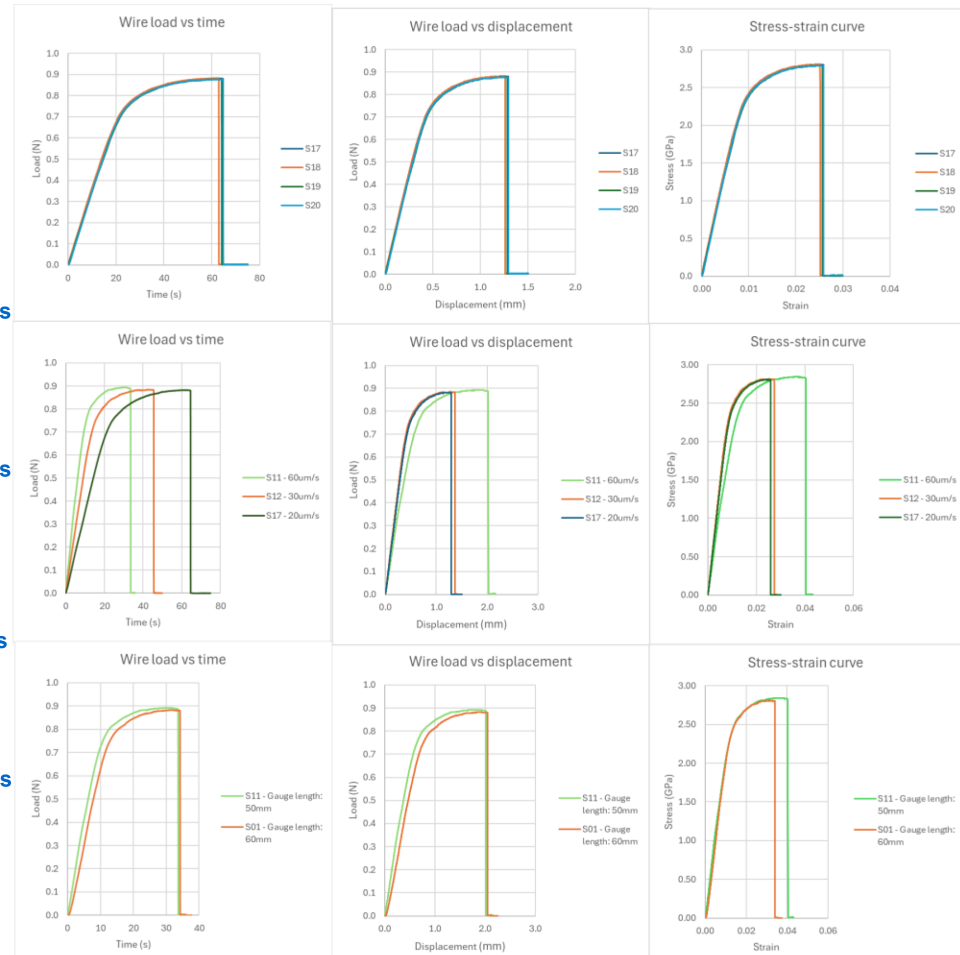

Typical values for this wire

- Tensile strength: 2000-3500 MPa
- Young's module: 250-310 GPa

N. De Filippis

Gold-plated tungsten wire

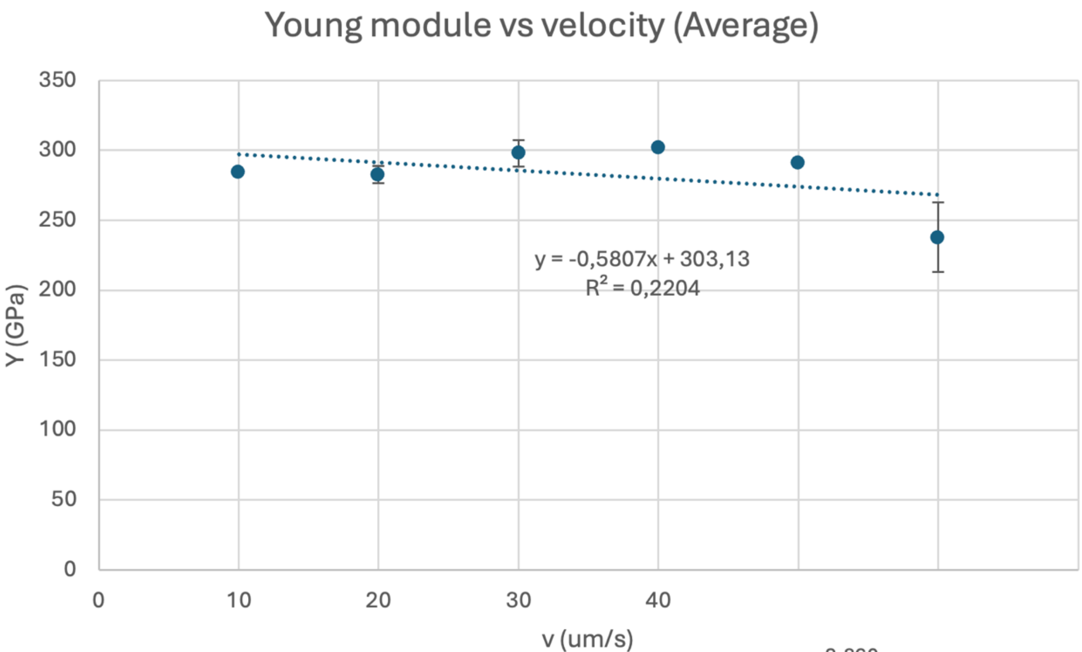

Slight dependence of the Young module from the velocity of the picometer

Slight increase of the Tensile Strenght with the velocity of the picometer

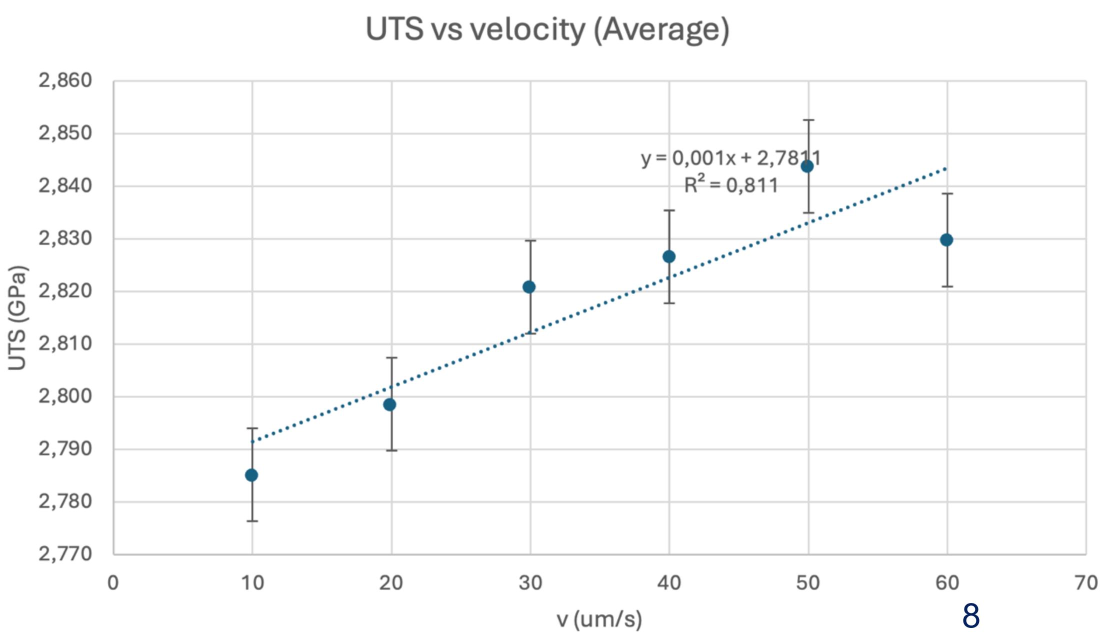

Gold-plated molibdenum wire

- Mo with Z=42 (lighter than W)
- 20 μm diameter wire
- conductive and easy to solder
- not as solid as the W

Specimen number	Tensile Strength - UTS (GPa)	Young module (Gpa)	R^2	Effective test time (s)	Total wire elongation (mm)	Elongation (%)	Fracture strain - ε_f (%)	Elongation at break (%)	Elastic limit strain - ε_y(%)	Yield Tensile Strength - YTS (GPa)
45	2.091	220.031	0.9992	51.675	1.034	2.067	0.021	2.067	0.005	1.098
46	2.107	226.061	0.9995	50.275	1.006	2.011	0.020	2.011	0.005	1.128
47	2.101	206.040	0.9979	54.175	1.084	2.167	0.022	2.168	0.005	1.028
48	2.110	222.461	0.9997	51.700	1.034	2.068	0.021	2.068	0.005	1.110
49	2.123	224.851	0.9993	53.075	1.062	2.123	0.021	2.123	0.005	1.122
Average Set	2.107	219.889	0.999	52.180	1.044	2.087	0.021	2.087	0.005	1.097

v=20 μm/s
l=50mm

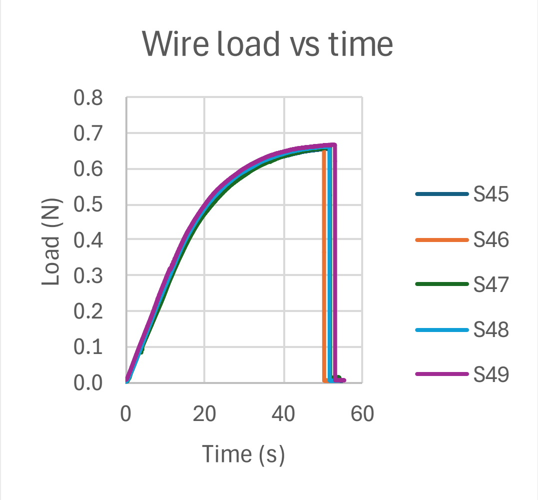

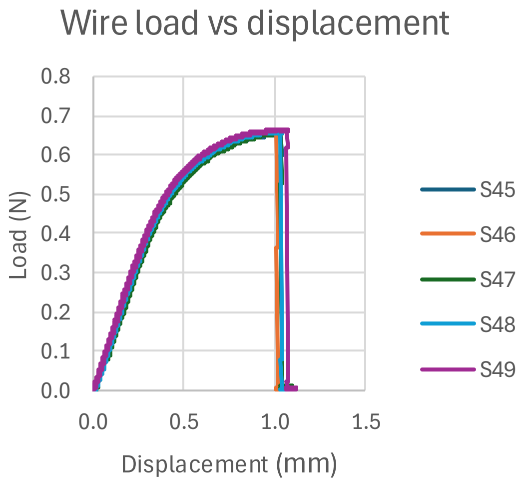

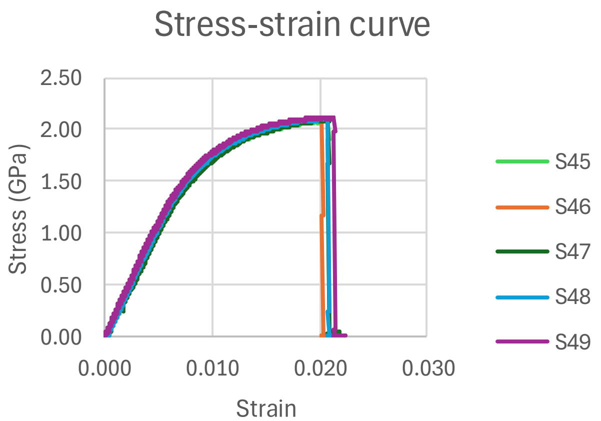

Carbon monofilament

- C with Z=6 (much lighter than W and Mo)
- 33.5 μm diameter wire
- not conductive → require coating
- easy to solder
- not as solid as the W

Purdue U. (US):
- coating / manufacturing facility at composite center Purdue would allow manufacturing all kinds of materials

Specimen number	Tensile Strength - UTS (GPa)	Young module (Gpa)	R^2	Effective test time (s)	Total wire elongation (mm)	Elongation (%)
21	1.445	103.413	0.9997	28.350	0.567	1.418
22	1.732	102.886	0.9996	33.725	0.675	1.686
23	2.120	103.973	0.9999	41.375	0.828	2.069
24	2.247	98.236	0.9986	45.650	0.913	2.283
25	2.247	107.915	0.9996	41.425	0.829	2.071
Average Set	1.958	103.284	0.999	38.105	0.762	1.905

v=20 μm/s
l=40mm

breaking

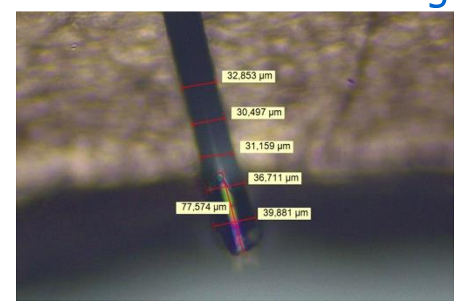

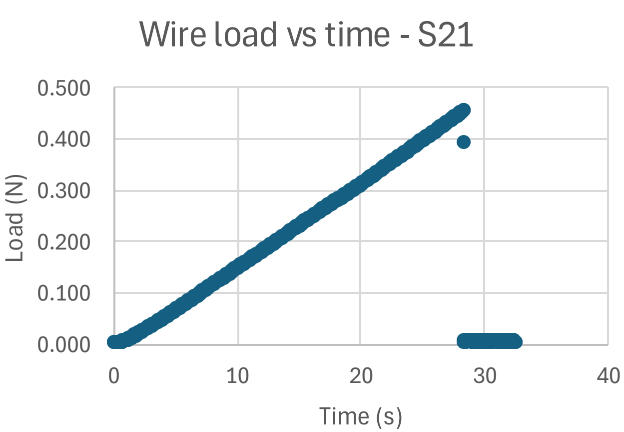

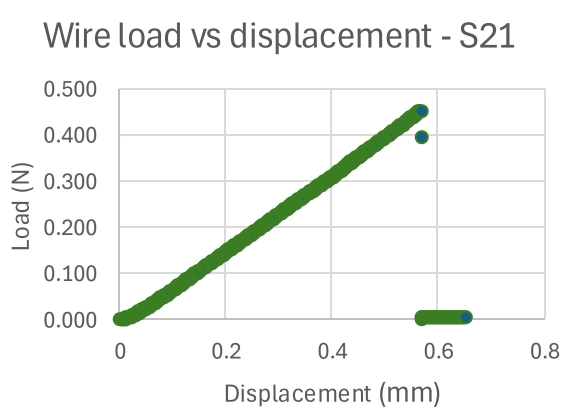

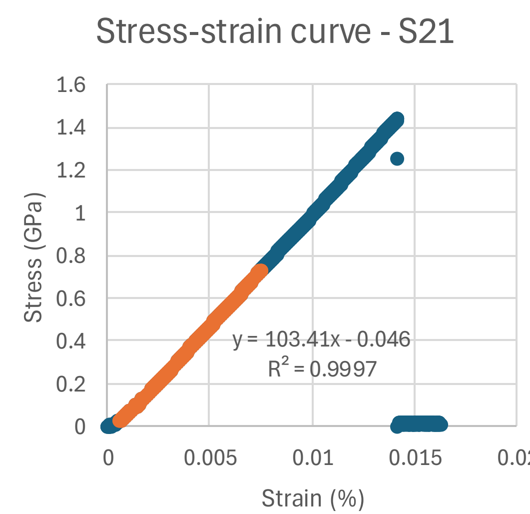

Challenges: minimization of the material budget

current
Material budget estimates

- Inner wall (from CMD3 drift chamber) — $8.4\times10^{-4}\ X_0$
  - 200 μm Carbon fiber
- Gas (from KLOE drift chamber) — $1.3\times10^{-3}\ X_0$
  - 90% He – 10% iC_4H_{10}
- Wires (from MEG2 drift chamber) — $1.3\times10^{-3}\ X_0$
  - 20 μm W sense wires $6.8\times10^{-4}\ X_0$
  - 40 μm Al field wires $4.3\times10^{-4}\ X_0$
  - 50 μm Al guard wires $1.6\times10^{-4}\ X_0$
- Outer wall (from Mu2e I-tracker studies) — $1.2\times10^{-2}\ X_0$
  - 2 cm composite sandwich (7.7 Tons)
- End-plates (from Mu2e I-tracker studies) — $4.5\times10^{-2}\ X_0$
  - wire cage + gas envelope
  - incl. services (electronics, cables, ...)

Mechanical structure of the DCH

New concept of construction allows to reduce material to $\approx 10^{-3} X_0$ for the barrel and to a few x $10^{-2} X_0$ for the end-plates.

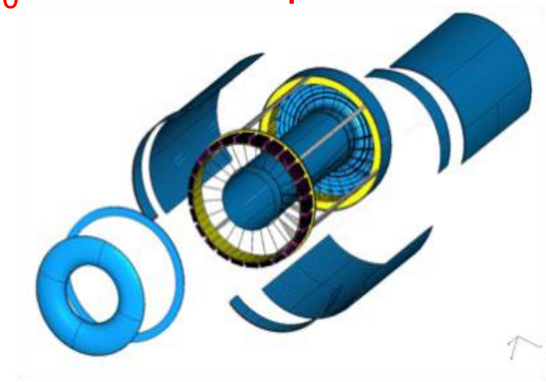

Gas containment
Gas vessel can freely deform without affecting the internal wire position and mechanical tension.

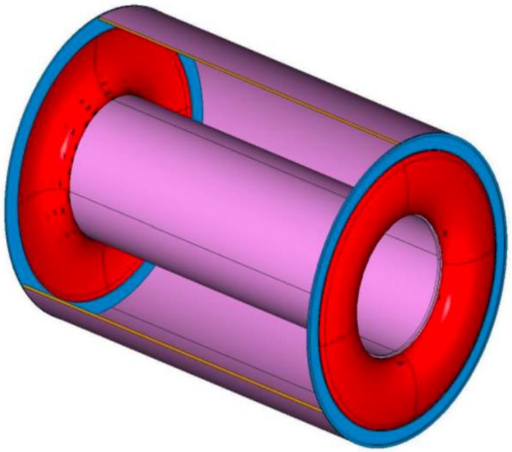

Wire cage
Wire support structure not subject to differential pressure can be light and feed-through-less

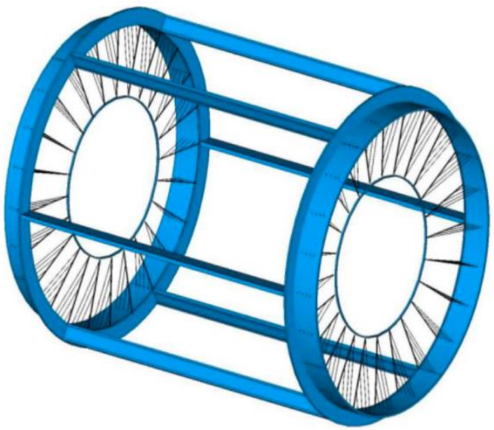

Mechanical structure of the DCH

- Outer cylinder made of 3 big panels 2cm thick made of 3 layers (2 monolithic CF with aluminum honeycomb structure in the middle)
- External and internal ring made of monolithic CF
- Endplates made of 48 Spokes (24 per endcap) forming 24 azimuthal sectors.
- Each spoke is supported by 15 Stays.
- Spoke length l = 165cm
- Inner cylinder wall thickness 200 μm CF (from CMD3 dch) – not structural

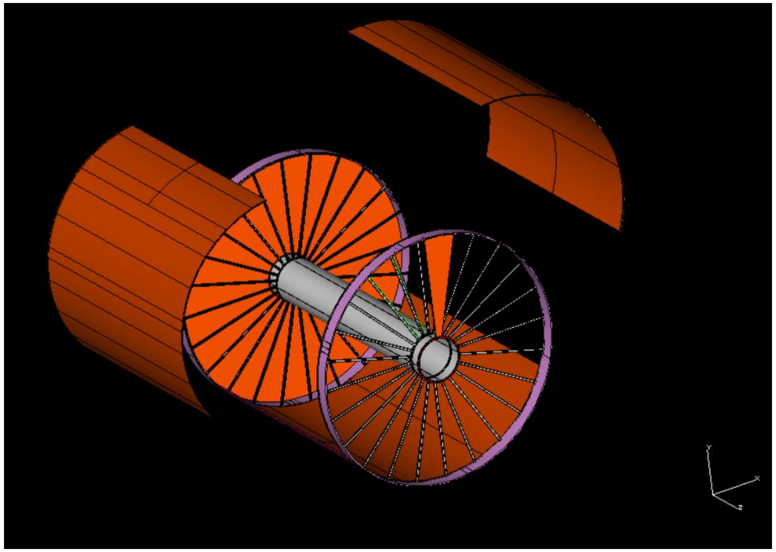

Big Problems to manage!

- σ_{xy} < **100 μm** → accuracy on the position of the anodic wires < **50 μm**.
- The anodic and cathodic wires should be parallel in space to preserve the constant electric field.
- A 20 μm tungsten wire, 4 m long, will bow about 400 μm at its middle point, if tensioned with a load of approximately 30 grams.

tension recovery system

30 gr tension for each wire → **10 tonnes** of total load on the **endcap**

Load on spokes (24 sectors): 416 Kg/spoke => 2.5 Kg/cm average

Load on stays (14 stays/spoke) - 416 Kg/14/sin 8.6° = 200 Kg/stay

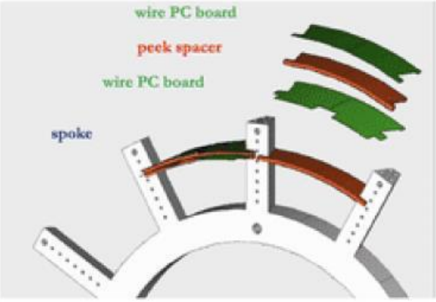

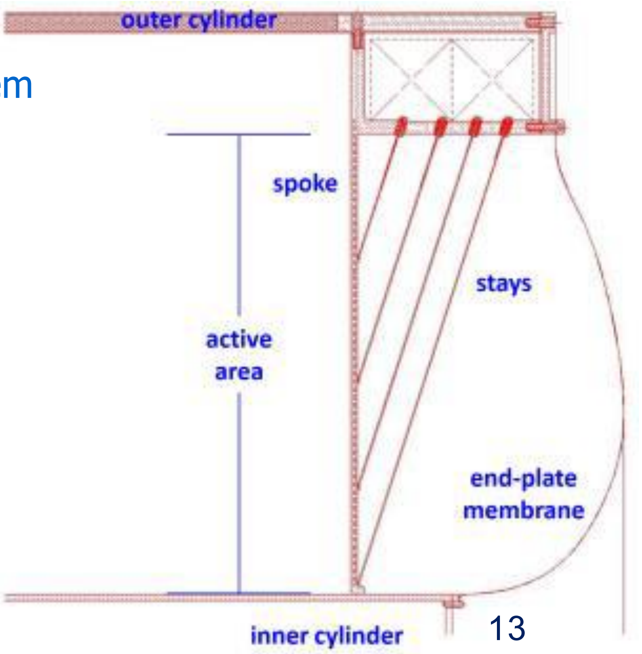

Mechanical structure with FEM: Example of prestressing

Goal: minimizing the deformation of the spokes

Materials:
- Epoxy-Carbon UD (395 GPa) Prepreg ➔ skins of the spoke
- Epoxy Carbon UD (230 GPa) Prepreg ➔ core of the spoke
- Aluminum Alloy ➔ inner and outer cylindrical walls

Loads & Boundary Conditions:
The effect of the PCBs' wire tension was defined as a pressure radially varying a from 0 to 0.159 MPa corresponding to a total load acting on the spoke of 444 kgf. Constraint fixed on top and bottom of spoke

Reaction forces:
The number of stays has been estimated in 15.
The reaction forces on these constraints are the vertical components of the tensile force each stay should apply to the spoke.

Result:
Such forces were applied to the system obtaining a directional **deformation of 0.19 mm** in its maximum value.

A possible improvement with pretension of the stays!

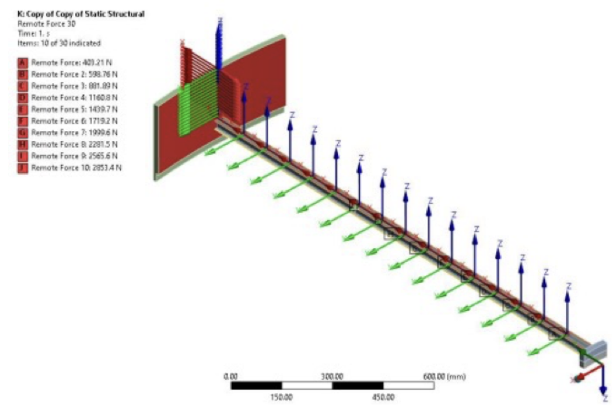

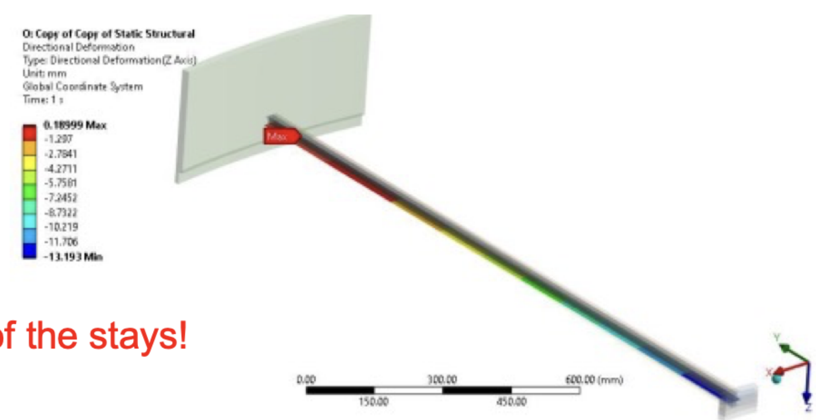

Vforce [N]	Hforce [N]
47.7	400.4
70.8	594.6
104.2	875.7
137.1	1152.7
169.9	1429.6
202.7	1707.2
235.4	1985.6
268.2	2265.7
301.1	2547.9
334.0	2833.8
367.1	3125.6
400.7	3430.7
440.6	3805.1
468.4	4116.5
499.9	4621.2

Mechanical structure with FEM: spokes production

- The core was milled with a numerically controlled machine.
- The winding foils were manually cut into strips of the sizes above.
- The PEEK side inserts were glued with acrylic adhesive.

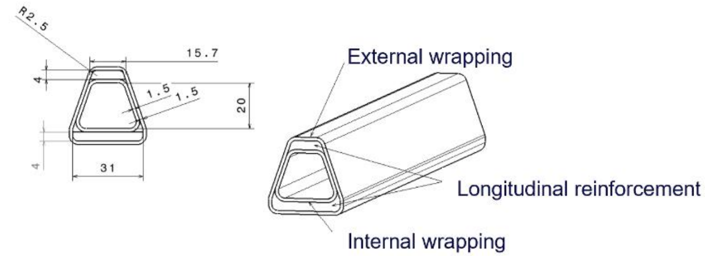

Item	Material	CPT (mm)	Layup	T (mm)
Internal wrapping	Prepreg Tissue 430g/m2	0.5	(0)3	1.5
Longitudinal reinforcement	Prepreg Tissue 800g/m2	0.86	(0)4	4
External wrapping	Prepreg Tissue 430g/m2	0.5	(0)3	1.5

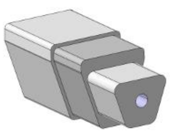

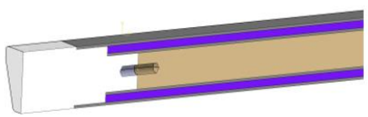

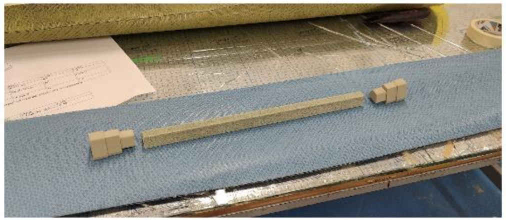

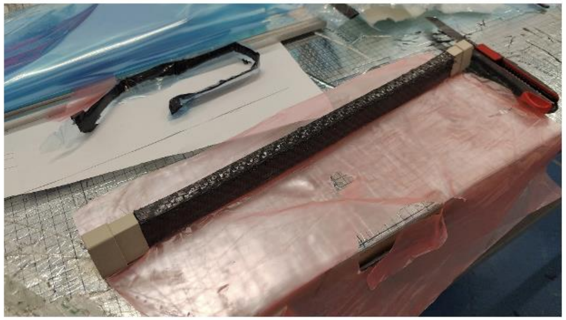

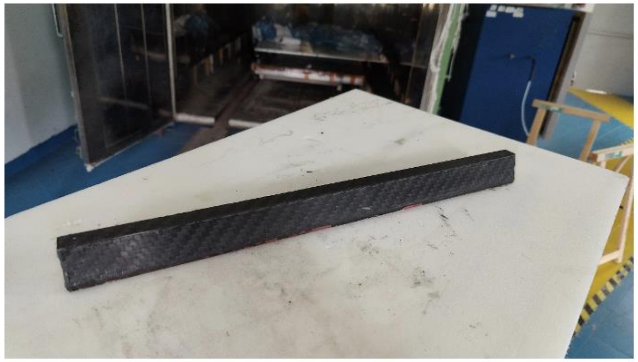

Mechanical structure: a complete model

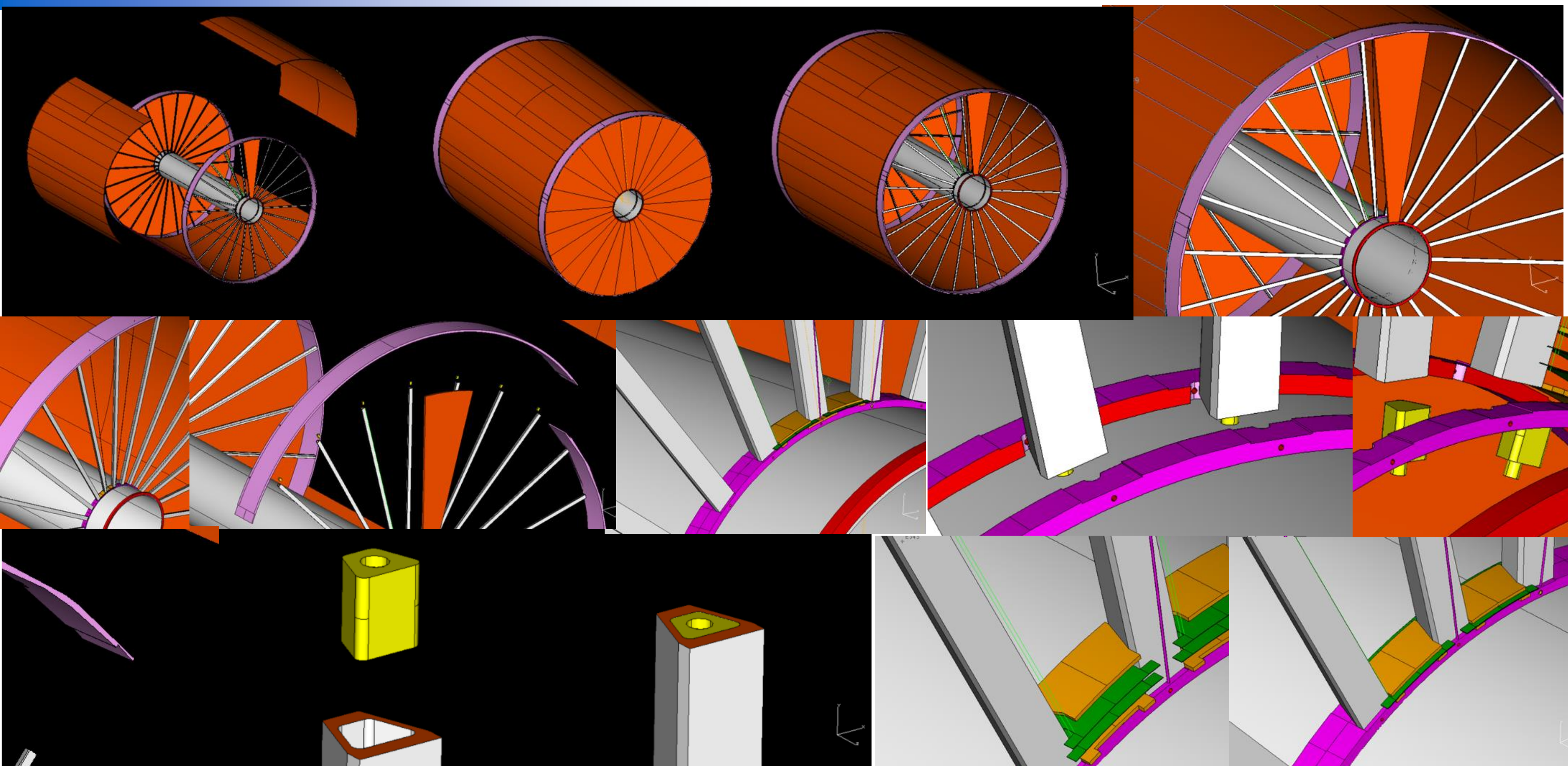

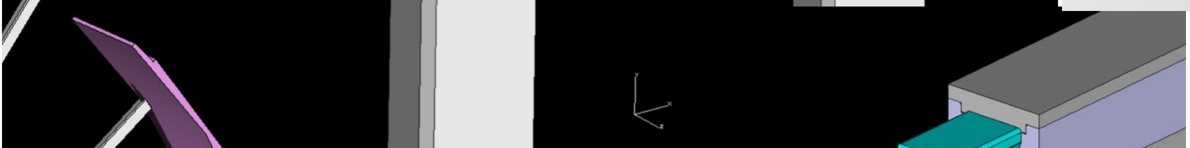

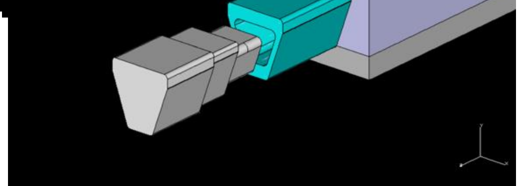

Started the construction of a DCH prototype full lenght, three sectors

A realistic complete model ready:

- mechanically accurate
- precise definition of the connections of the cables on the structure
- connections of the wires on the PCB
- location of the necessary spacers
- connection between wire cage and gas containment structure

2025 full-length prototype: Goals

- ▸ **Check the limits of the wires' electrostatic stability at full length and at nominal stereo angles**

- ▸ **Test different wires**: uncoated Al, C monofilaments, Mo sense wires, …, of different diameters
  - Test different wire anchoring procedures (soldering, welding, gluing, crimping, …) to the wire PCBs
  - Test different materials and production procedures for spokes, stays, support structures and spacers
  - Test compatibility of proposed materials with drift chamber operation (outgassing, aging, creeping, …)

- ▸ Validate the **concept of the wire tension recovery scheme** with respect to the tolerances on the wire positions
  - Optimize the layout of the wires' PCBs (sense, field and guard), according to the wire anchoring procedures, with aim at minimizing the end-plate total material budget

- ▸ Starting from the new concepts implemented in the MEG2 DCH robot, **optimize the wiring strategy**, by taking into account the 4m long wires arranged in multi-wire layers

- ▸ Define and validate **the assembly scheme** (with respect to mechanical tolerances) of the multi-wire layers on the end plates
  - Define the front-end cards channel multiplicity and their location (cooling system necessary?)

- ▸ **Optimize the High Voltage and signal distribution** (cables and connectors)

- ▸ Test performance of **different versions of front-end, digitization and acquisition chain**

▸ ***Full-length prototype necessary***

○ ***Can be done in parallel on small prototypes***

2025 full-length prototype: Wiring

Target: a full length DCH prototype with 3 sectors per endcap

- 8 spokes (4 per endcap)
- Internal ring
- part of the outer ring
- part of the cylindrical panel

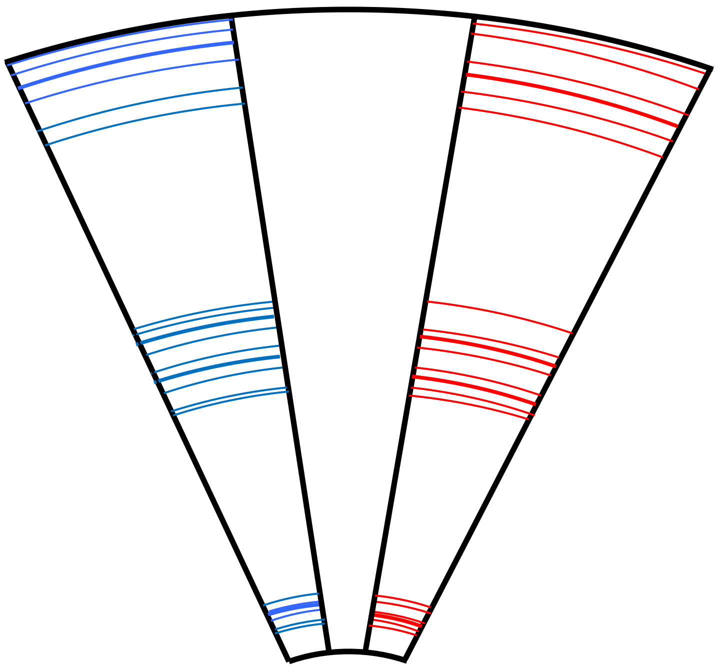

First two layers of superlayer #1
V and U guard layers (2 x 9 guard wires)
V and U field layers (2 x 18 field wires)
U layer (8 sense + 9 guard)
U and V field layers (2 x 18 field wires)
V layer (8 sense + 9 guard)
V and U field layers (2 x 18 field wires)
V and U guard layer (2 x 9 guard wires)

Last two layers of superlayer #7
V and U guard layers (2 x 21 guard wires)
V and U field layers (2 x 42 field wires)
U layer (20 sense + 21 guard)
U and V field layers (2 x 42 field wires)
V layer (20 sense + 21 guard)
V field layer (42 field wires)

First two layers of superlayer #8
U field layer (46 field wires)
U layer (22 sense + 23 guard)
U and V field layers (2 x 46 field wires)
V layer (22 sense + 23 guard)
V and U field layers (2 x 46 field wires)
V and U guard layer (2 x 23 guard wires)

Last two layers of superlayer #14
V and U guard layers (2 x 35 guard wires)
V and U field layers (2 x 70 field wires)
U layer (34 sense + 35 guard)
U and V field layers (2 x 70 field wires)
V layer (34 sense + 35 guard)
V and U field layers (2 x 70 field wires)
V and U guard layer (2 x 35 guard wires)

TOTAL LAYERS: 8
Sense wires: 168
Field wires: 965
Guard wires: 264

PCBoards wire layers: 42
Sense wire boards: 8
Field wire boards: 22
Guard wire boards: 12
HV values: 14

Readout channels: 8+8 +16+16+16+16 + 16+16 = 112

2025 full-length prototype: Coverage

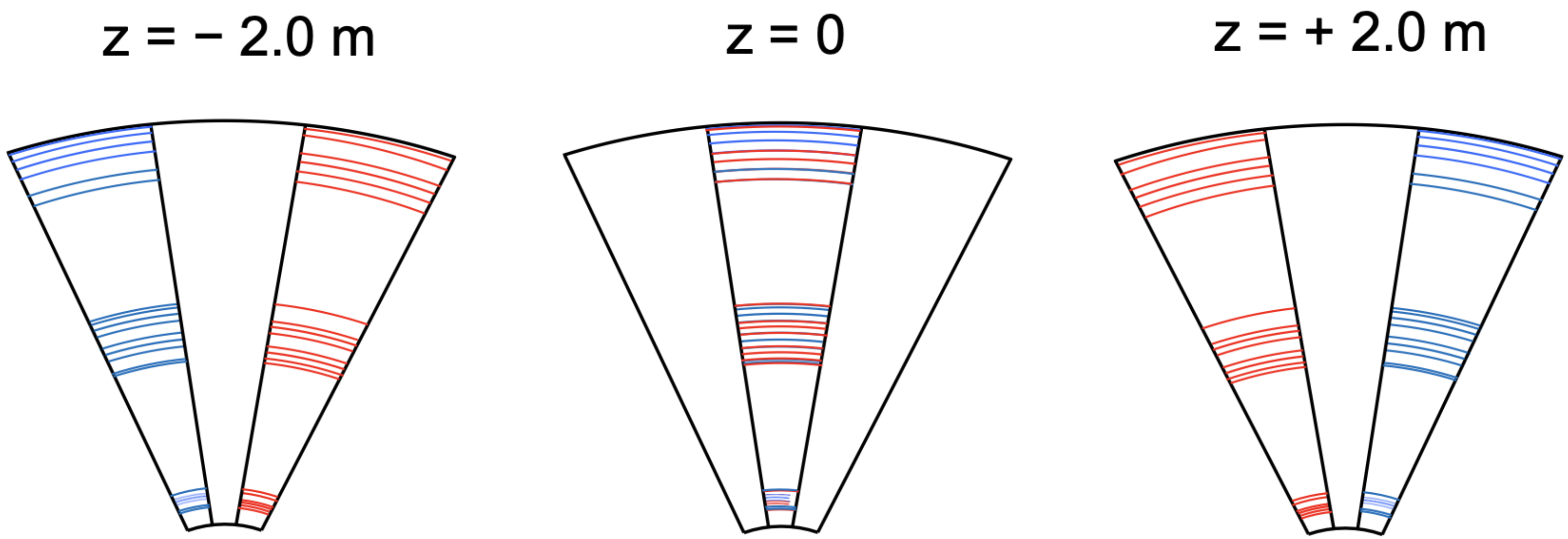

MAX COVERAGE

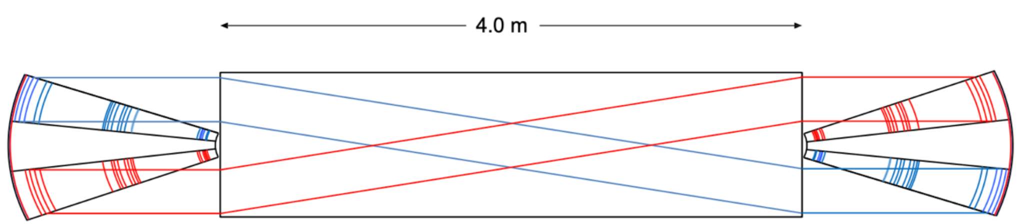

ELECTRONICS COVERAGE

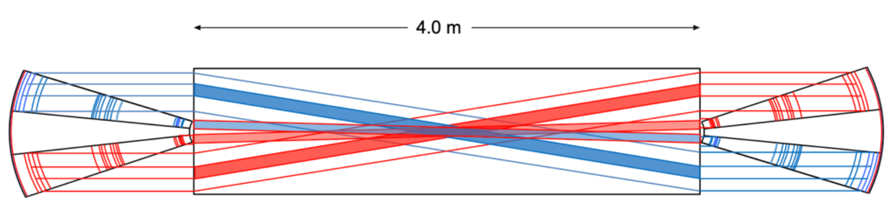

Minimum stereo angle 50 mrad
Maximum stereo angle: 250 mrad

Testbeam data analysis

The Drift Chamber: Cluster Counting/Timing and PID

Principle: In He based gas mixtures the signals from each ionization act can be spread in time to few ns. With the help of a fast read-out electronics they can be identified efficiently.

- By counting the number of ionization acts per unit length (dN/dx), it is possible to identify the particles (P.Id.) with a better resolution w.r.t the dE/dx method.

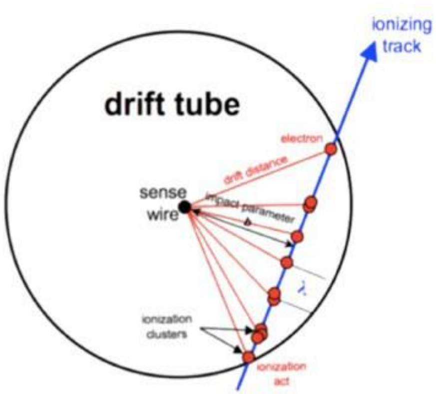

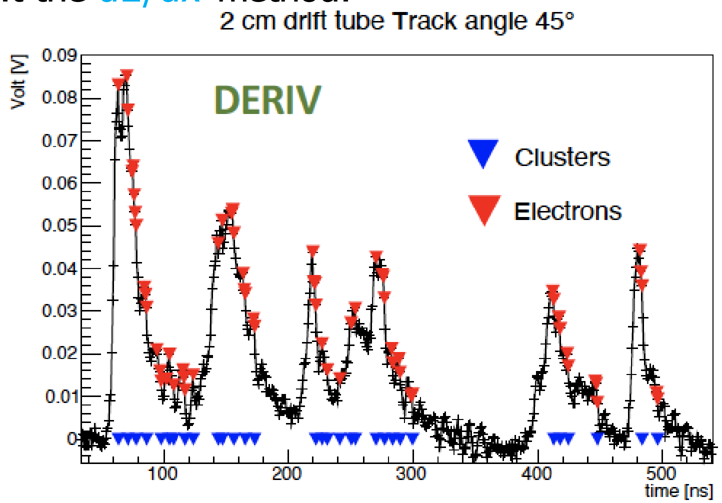

- collect signal and identify peaks
- record the time of arrival of electrons generated in every ionisation cluster
- reconstruct the trajectory at the most likely position

Requirements
fast front-end electronics
(**bandwidth ~ 1 GHz**)
high sampling rate digitization
(**~ 2 GSa/s, 12 bits, >3 KB**)

- Landau distribution of dE/dx originated by the mixing of primary and secondary ionizations, has large fluctuations and limits separation power of PID → primary ionization is a Poisson process, has small fluctuations

- The cluster counting is based on replacing the measurement of an ANALOG information (the [truncated] mean dE/dX) with a DIGITAL one, the number of ionisation clusters per unit length:

dE/dx: truncated mean cut (70-80%), with a 2m track at 1 atm give $\sigma \approx 4.3\%$

dN_{cl}/dx: for He/iC_4H_{10}=90/10 and a 2m track gives $\sigma_{dNcl/dx}$ **/(dN_{cl}/dx)** < 2.0%

Beam tests in 2021,2022, 2023 and 2024

Beam tests to experimentally asses and optimize the **performance of the cluster counting/timing** techniques:

- Two **muon beam tests** performed at **CERN-H8** (**$\beta\gamma > 400$**) in Nov. 2021 and July 2022 (p_T = 165/180 GeV).
- A **muon beam test** (from 4 to 12 GeV momentum) in 2023 performed at **CERN**. A new testbeam with the same configuration done on July 10, 2024
- Ultimate test at **CERN**/**FNAL-MT6** in 2026 with □ and **K ($\beta\gamma$ = 10−140)** to fully exploit the relativitic rise.

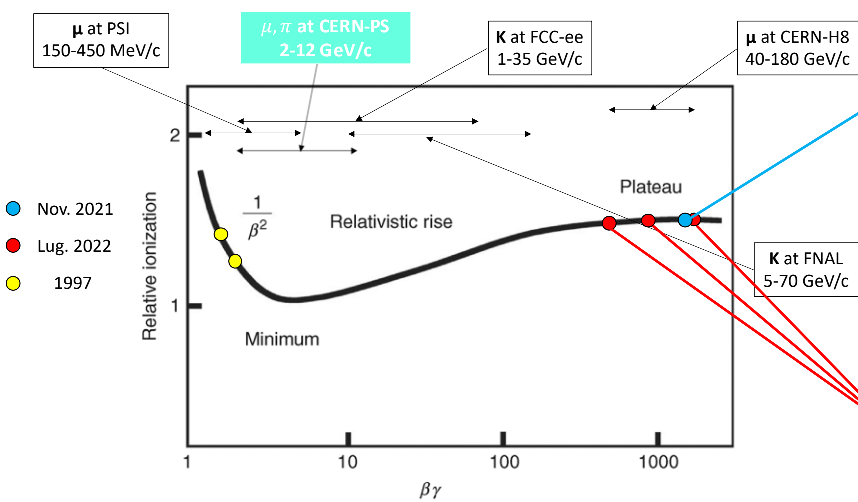

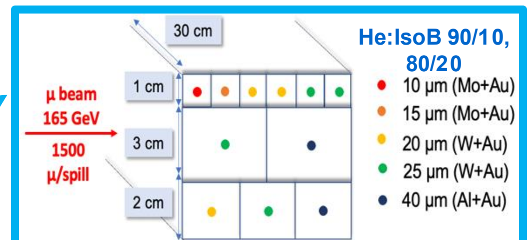

90%He-10%iC_4H_{10}
nominal HV+20, 45°,
Gas gain ~ $2 \cdot 10^5$,
165 GeV/c

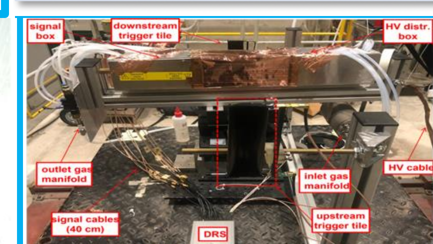

2021/2022 beam test results: performance plots

Several algorithms developed for electron peak finding:

- ✓ Derivative Algorithm (DERIV)
- ✓ and Running Template Algorithm (RTA)
- ✓ NN-based approach (developed by IHEP)
- ▪ Clusterization algorithm to merge electron peaks in consecutive bins
- ▪ Poissonian distribution for the number of clusters as expected
- ▪ Different scans have been done to check the performance: (HV, Angle, gas gain, template scan)

Sense Wire Diameter 15 μm; Cell Size 1.0 cm
Track Angle 45; Sampling rate 2 GSa/s
Gas Mixture He:IsoB 80/20

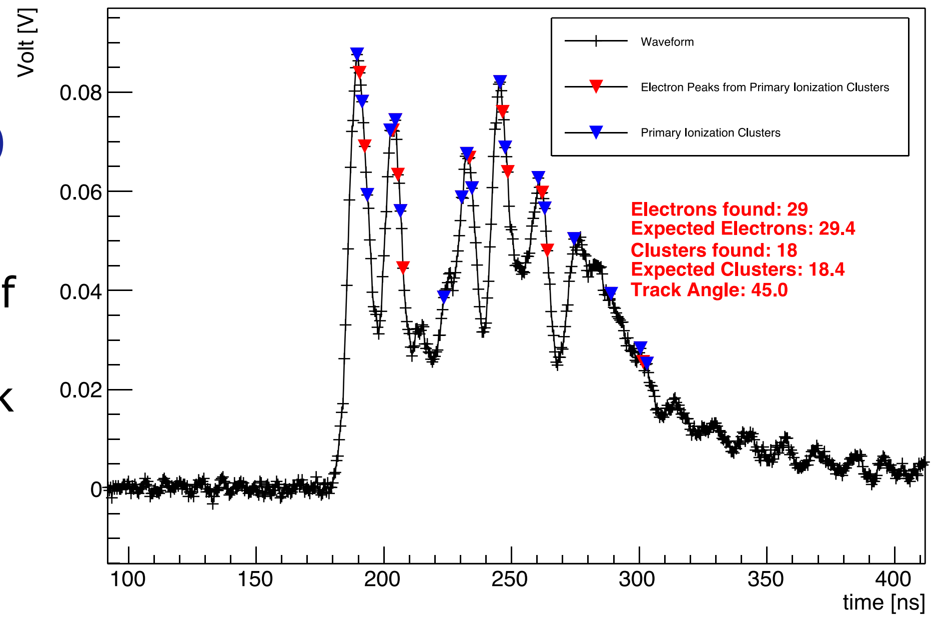

Expected number of electrons =
δ cluster/cm (M.I.P.) * drift tube size [cm] * 1.3 (relativistic rise)* 1.6 electrons/cluster * 1/cos(α)

- α = angle of the muon track w.r.t. normal direction to the sense wire
- δ cluster/cm (M.I.P) changes from 12, 15, 18 respectively for He:IsoB 90/10, 85/15 and 80/20 gas mixtures.
- drift tube size are 0.8, 1.2, and 1.8 respectively for 1 cm, 1.5 cm, and 2 cm cell size tubes.

Poissonian distribution for the number of clusters

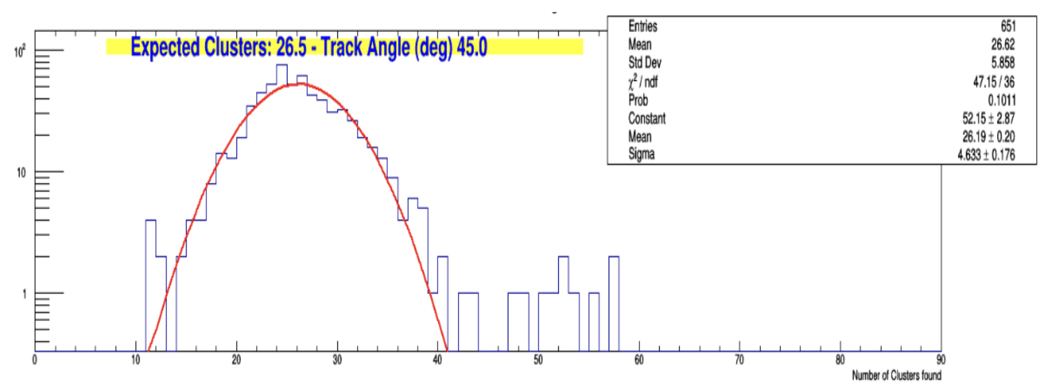

[1] H. Fischle, J. Heintze and B. Schmidt, Experimental determination of ionization cluster size distributions in counting gases, NIMA 301 (1991)

2021/2022 beam test results: performance plots

dE/dx Resolution

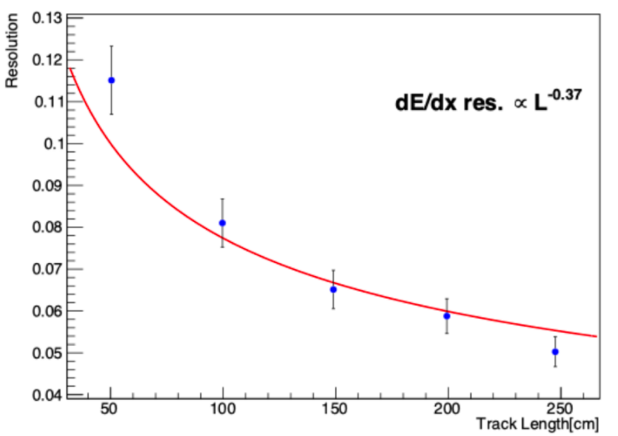

dE/dx resolution dependence on the track length $L^{-0.37}$

dN/dx Resolution

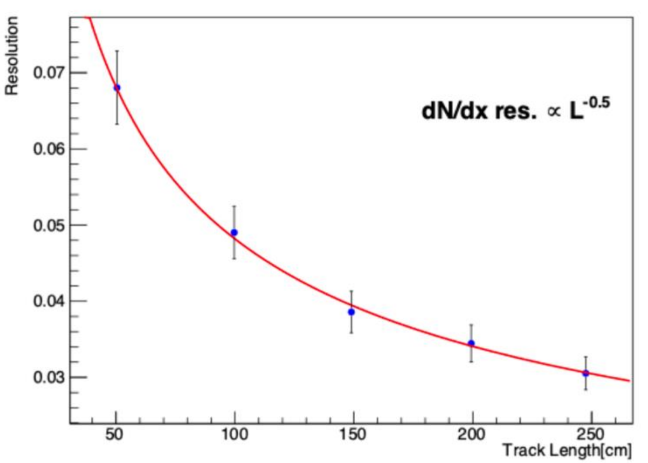

Paper submitted to JINST
https://arxiv.org/abs/2509.21883

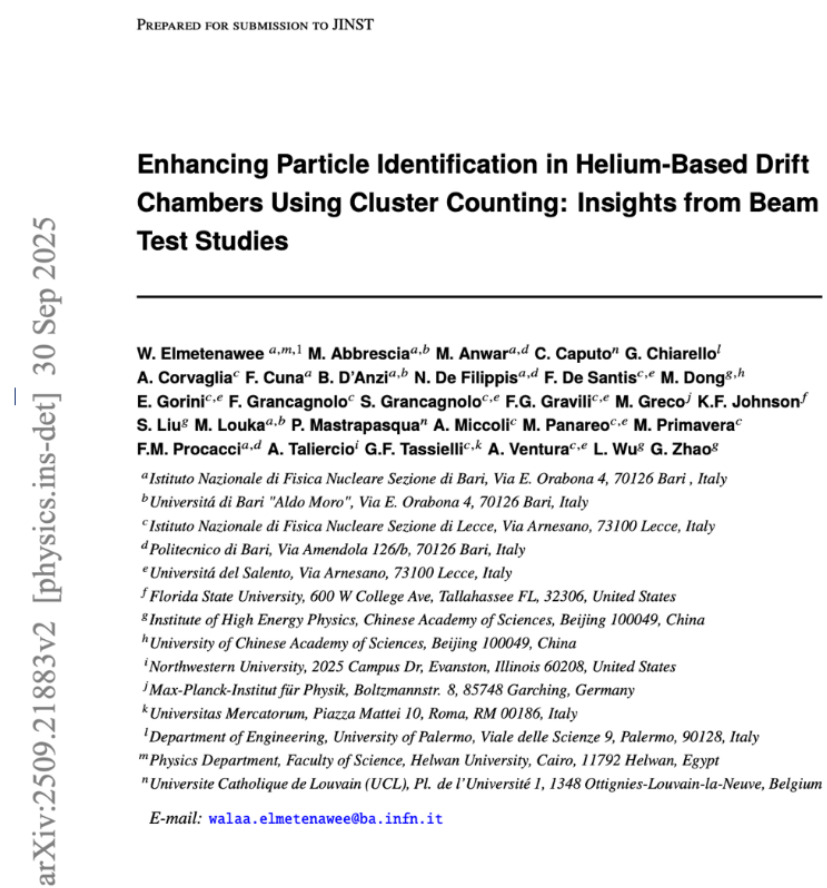

Prepared for submission to JINST

arXiv:2509.21883v2 [physics.ins-det] 30 Sep 2025

Enhancing Particle Identification in Helium-Based Drift Chambers Using Cluster Counting: Insights from Beam Test Studies

W. Elmetenawee [a,m,1] M. Abbrescia[a,b] M. Anwar[a,d] C. Caputo[n] G. Chiarello[l]
A. Corvaglia[c] F. Cuna[a] B. D'Anzi[a,b] N. De Filippis[a,d] F. De Santis[c,e] M. Dong[g,h]
E. Gorini[c,e] F. Grancagnolo[c] S. Grancagnolo[c,e] F.G. Gravili[c,e] M. Greco[j] K.F. Johnson[f]
S. Liu[g] M. Louka[a,b] P. Mastrapasqua[n] A. Miccoli[c] M. Panareo[c,e] M. Primavera[c]
F.M. Procacci[a,d] A. Taliercio[i] G.F. Tassielli[c,k] A. Ventura[c,e] L. Wu[g] G. Zhao[g]

[a] *Istituto Nazionale di Fisica Nucleare Sezione di Bari, Via E. Orabona 4, 70126 Bari , Italy*
[b] *Universitá di Bari "Aldo Moro", Via E. Orabona 4, 70126 Bari, Italy*
[c] *Istituto Nazionale di Fisica Nucleare Sezione di Lecce, Via Arnesano, 73100 Lecce, Italy*
[d] *Politecnico di Bari, Via Amendola 126/b, 70126 Bari, Italy*
[e] *Universitá del Salento, Via Arnesano, 73100 Lecce, Italy*
[f] *Florida State University, 600 W College Ave, Tallahassee FL, 32306, United States*
[g] *Institute of High Energy Physics, Chinese Academy of Sciences, Beijing 100049, China*
[h] *University of Chinese Academy of Sciences, Beijing 100049, China*
[i] *Northwestern University, 2025 Campus Dr, Evanston, Illinois 60208, United States*
[j] *Max-Planck-Institut für Physik, Boltzmannstr. 8, 85748 Garching, Germany*
[k] *Universitas Mercatorum, Piazza Mattei 10, Roma, RM 00186, Italy*
[l] *Department of Engineering, University of Palermo, Viale delle Scienze 9, Palermo, 90128, Italy*
[m] *Physics Department, Faculty of Science, Helwan University, Cairo, 11792 Helwan, Egypt*
[n] *Universite Catholique de Louvain (UCL), Pl. de l'Université 1, 1348 Ottignies-Louvain-la-Neuve, Belgium*

E-mail: walaa.elmetenawee@ba.infn.it

~ 2 times improvement in the resolution using dN/dx method

Garfield fast/full simulation chain

IHEP + M. Anwar/N. De Filippis (Bari Politecnico)

Courtesy of. G. Zhao et al (IHEP)

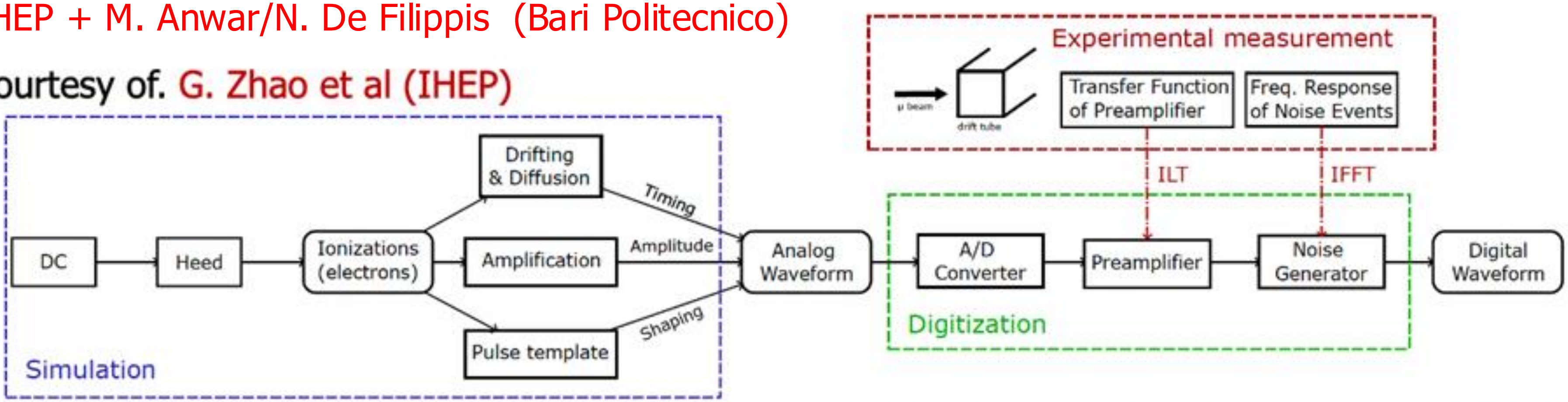

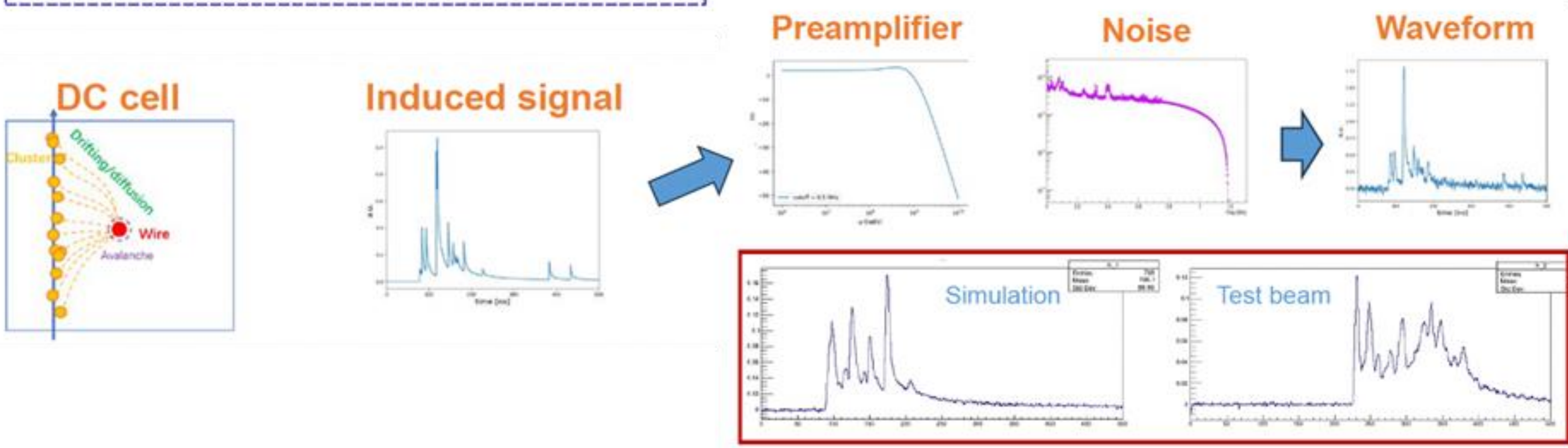

"Peak finding algorithm for cluster counting with domain adaptation"

Comp. Phys. Comm., 300, 2024, 109208, https://doi.org/10.1016/j.cpc.2024.109208

NN-based algorithms

Peak finding with LSTM(*)

Why LSTM? Waveforms are time series

- Architecture: LSTM (RNN-based)
- Method: Binary classification of signals and noises on slide windows of peak candidates

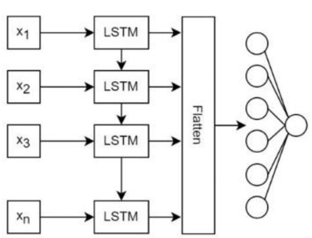

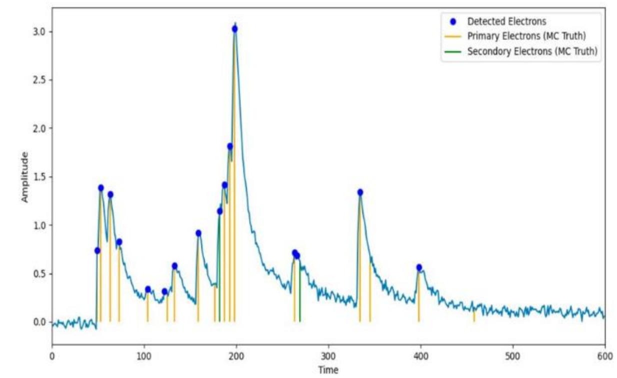

Clusterization with DGCNN(**)

Why DGCNN? Locality of the electrons in the same primary cluster, perform message-passing through neighbour nodes in GNN.

- Architecture: DGCNN (GNN-based)
- Method: Binary classification of primary and secondary electrons

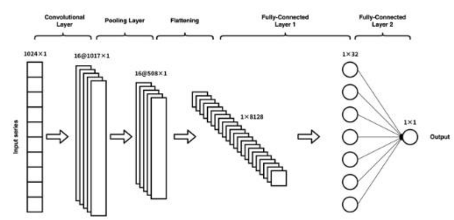

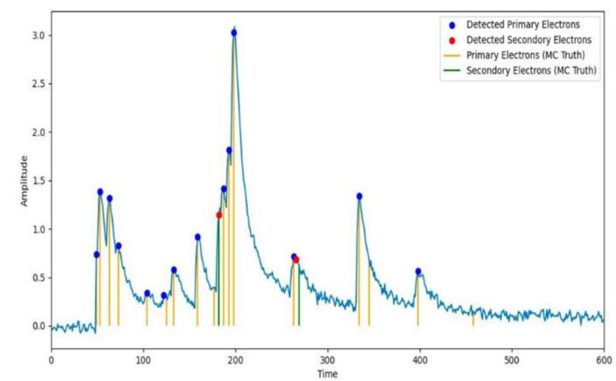

(*) LSTM: Long Short-Term Memory

(**) DGCNN: Dynamic Graph Convolutional neural networks

NN-based algorithms

Different Momenta of Muon (GeV)	2	4	6	8	10	180
Monte Carlo (MC)						
Primary Cluster (MC)	15.89	16.99	17.81	18.28	18.53	19.10
Std. Deviation (MC)	4.01	4.10	4.12	4.30	4.20	4.30
LSTM Model						
Primary Cluster (LSTM)	14.45	15.37	16.06	16.34	16.49	17.30
Std. Deviation (LSTM)	3.77	3.84	3.90	3.90	3.90	4.02
CNN Model						
Primary Cluster (CNN)	14.38	15.00	15.38	15.77	16.29	16.76
Std. Deviation (CNN)	3.37	3.20	3.20	3.10	3.30	3.20

Table 1: Primary cluster means and standard deviations from MC, LSTM, and CNN across different muon momenta.

Mean number of primary clusters at 10 GeV muon momentum

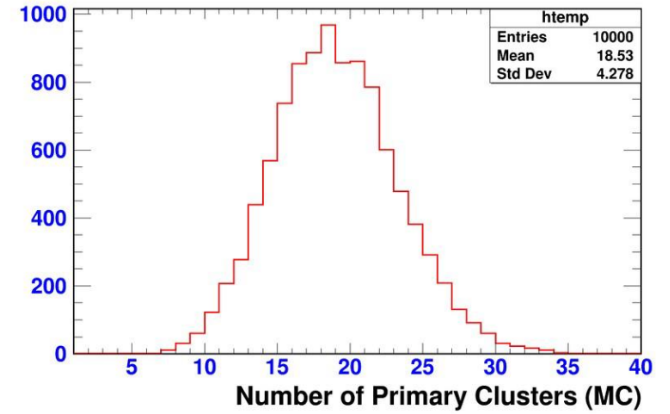

- working on comparing simulation with real data from test beams
- tuning the simulation to compare with data
- use NN to infer the number of cluster for any waveform
- new strategy for digitization on going

→ Stay tuned

DRD1: Gas Detectors

WP2 - Inner and central tracking with PID (Drift Chambers)

Task ID	Task	Performance Goal	ECFA DRD Theme
T1	Development of front-end ASIC for cluster counting	Design/construction/test of a prototype of the frontend ASIC for cluster counting (with High bandwidth, High gain, Low power consumption, Low mass)	1.1, 1.2, 1.3
T2	Development of a scalable multichannel DAQ board	Working prototype of a scalable multichannel DAQ board (with High sampling rate, Dead-time-less, DSP and filtering ability, Event time stamping, for Track triggering)	
T3	Mechanics: new wiring procedures and new endplate concepts	Conceptual designs of novel wiring procedures (feed-through-less wiring procedures) and full design of innovative concepts of more transparent endplate (< 5% X_0).	
T4	Increase rate capability and granularity	Measurements of performance on prototypes of drift cells at different granularities (smaller cell size and shorter drift time) and with different field configurations (higher field-to-sense ratio).	
T5	Consolidation of new wire materials and wire metal coating	Evaluation of the electrostatic stability of wires with High yield strength, Low mass, low Z, High conductivity. Study of aging effects. Evaluation of existing or a sputtering facility for metal coating of carbon wires.	
T6	Study ageing phenomena for new wire types	Tests of prototypes built with new wire types at beams and irradiation facilities. Measurement of performance on total integrated charge and establish charge collection limits.	
T7	Optimization of gas mixing, recuperation, purification and recirculation systems	Measurement of the performance of hydrocarbon-free gas mixtures with High quenching power, Low-Z, High radiation length. Design of a recirculating system.	

STARTED

STARTED

ADVANCED

TO BE RESTARTED

STARTED

TO BE STARTED

NOT STARTED

Summary/Conclusions

Good progress reported on:

- mechanical structure design → NEW results
- on going effort to build a full-length prototype next year
- testbeam data analysis → NEW results

Plenty of areas for collaboration (also in the context of DRD1 WP2):

- detector design, construction, beam test, performance
- local and global reconstruction, full simulation
- physics performance and impact
- etc.

Effort to build a international collaboration enforced

- well established collaboration with IHEP for NN-based cluster counting algorithms and IJCLAB
- started to collaborate with US people from BNL and Purdue

Backup

Design features of the IDEA Drift Chamber

For the purpose of tracking and ID at low and medium momenta mostly for heavy flavour and Higgs decays, the IDEA drift chamber is designed to cope with:

- transparency against multiple scattering, more relevant than asymptotic resolution
- a high precision momentum measurement
- an excellent particle identification and separation

IDEA: Material vs. cos(θ)

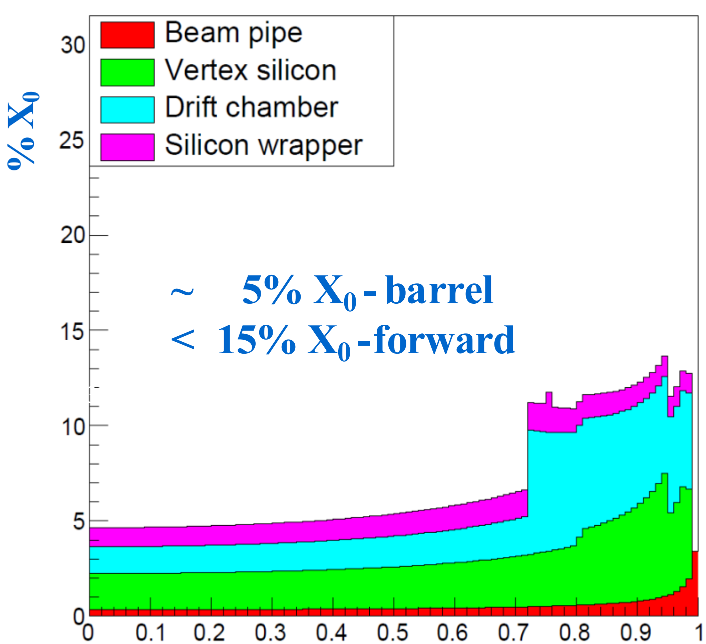

σ_{pt}/pt

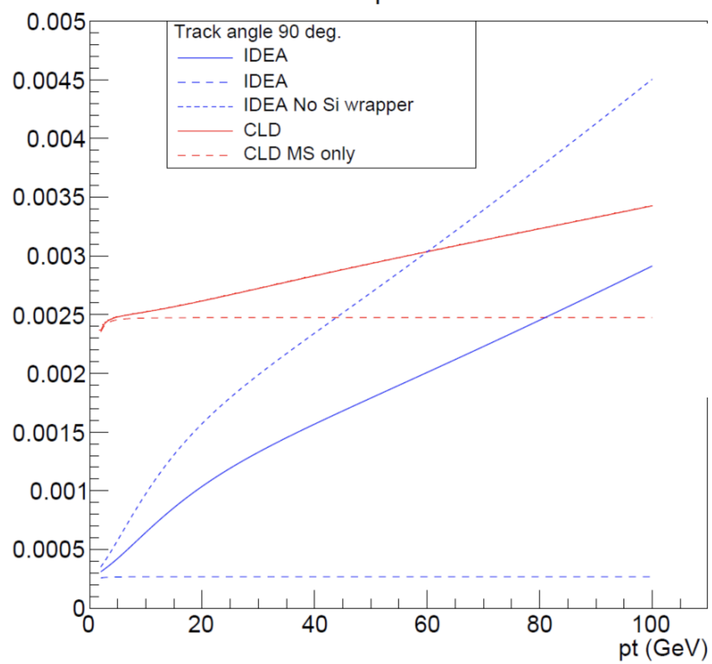

Particle momentum range far from the asymptotic limit where MS is negligible

$$\frac{\Delta p_T}{p_T}\Big|_{res.} \approx \frac{12\,\sigma_{r\phi}\,p_T}{0.3\,B_0 L_0^2}\sqrt{\frac{5}{N+5}}$$

$$\frac{\Delta p_T}{p_T}\Big|_{m.s.} \approx \frac{0.0136\,\mathrm{GeV/c}}{0.3\beta\,B_0 L_0}\sqrt{\frac{d_{tot}}{X_0\,\sin\theta}}$$

Drasal, Riegler, https://doi.org/10.1016/j.nima.2018.08.078

For 10 GeV (50 GeV) μ emitted at an angle of 90° w.r.t the detector axis, the p_T resolution is

- about 0.05 % (0.15%) with the very light IDEA DCH

Wire tests: definitions and procedures

- L = load (in N) measured with the dynamometer
- t = time (in s) measured with the slider
- A = filament area (m^2)
- v = picomotor velocity (in µm/s)
- D = displacement (in mm) = v*t
- SS = stress (in Gpa) = L/A
- ST = strain (in %) = D/GL
- GL = gauge length (mm)
- TS = Tensile Strength (in GPa) = Max(SS)
- Y = Young module (Gpa) from the slope of the elastic part of Stress-Strain curve
- R^2= correlation coefficient
- Effective test time (s) = the time up to the break
- TWE Total wire elongation (mm) = the elongation up to the break
- Elongation (%) = TWE/GL*100
- Fracture strain - εf (%), value of the strain at the break point
- Elongation at break (%) = εf *100
- Elastic limit strain - εy(%), value of the strain at the end of elastic part
- Yield Tensile Strength - YTS (GPa) = Y* εy

Mechanical structure: FEM simulation studies

Simulation studies: progress about the final design of the cross section of the spoke

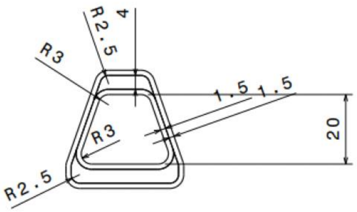

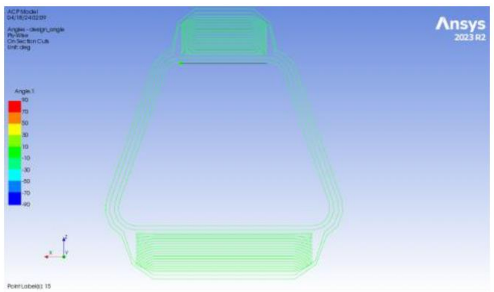

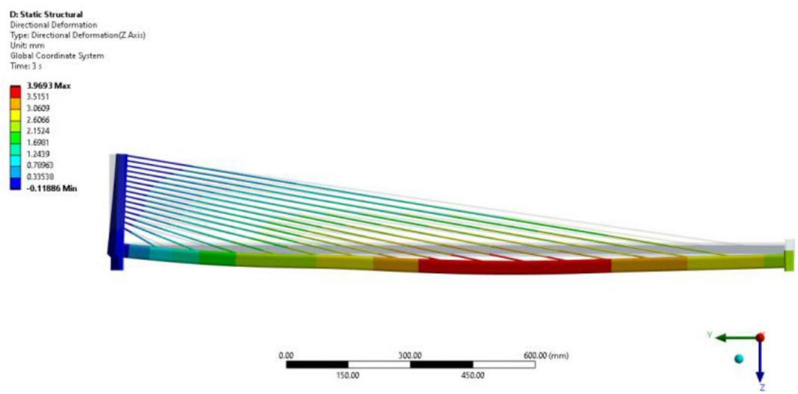

Statical structure simulation:

deformation along r

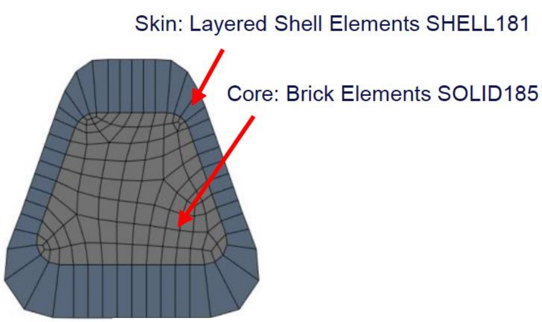

Our main goal is to limit the deformation of the spokes to **200 μm**, while ensuring the structural integrity

- Including **prestressing of spokes**
- Investigate more **composite structures**

- **Buckling** analysis on outer cylinder

Mechanical desing for DCH with FEM analysis

- The structural parts of the drift chamber mechanics will be built in carbon fibre.

- Spoke manufacturing technique influences the individuation of more performant cross sections

1^{st} CHALLENGES: wire types – Carbon monofilament

SPECIALTY MATERIALS, INC.

Manufacturers of Boron and SCS Silicon Carbide Fibers and Boron Nanopowder

CARBON MONOFILAMENT

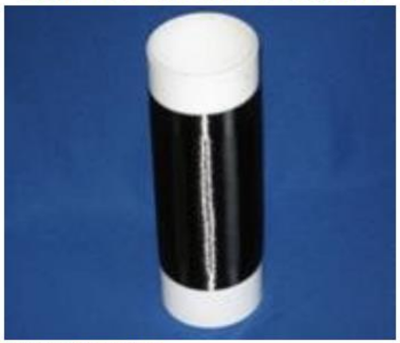

TYPICAL PROPERTIES

Diameter:	0.00136 +/- 0.0001" (34.5 +/- 2.5 µm)	
Tensile Strength:	125 ksi (0.86 GPa)	0.65 GPa
Tensile Modulus:	6 msi (41.5 GPa)	
Electrical Resistivity:	3.6 x 10^{-3} ohm cm	37 KΩ/m
Density:	1.8 g/cc	

Specialty Materials, Inc.
1449 Middlesex Street
Lowell, Massachusetts 01851

Phone: 978-322-1900
Fax: 978-322-1970

CARBON MONOFILAMENT PRODUCT PRICE LIST
Effective October 1, 2017

Product	Quantity	Price LF
CARBON MONOFILAMENT	1 Million LF	$0.02
	500,000 LF	$0.03
	1,000 LF	$0.93

CARBON MONOFILAMENT PRODUCT PRICE LIST EFFECTIVE APRIL 1, 2019

Product	Quantity	Price per LF	
CARBON MONOFILAMENT	1 Million LF	$0.02	60 €/Km
	500,000 LF	$0.03	
	1,000 LF	$0.94	

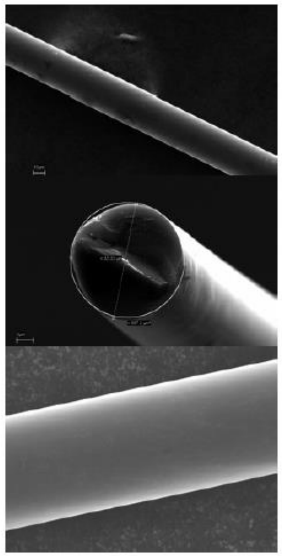

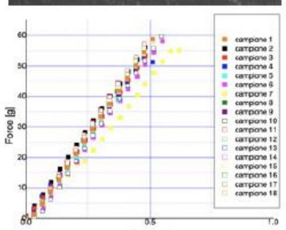

Metal coating by HiPIMS: High-power impulse magnetron sputtering

physical vapor deposition (PVD) of thin films based on magnetron sputter deposition (extremely high power densities of the order of kW/cm² in short pulses of tens of microseconds at low duty cycle <10%)

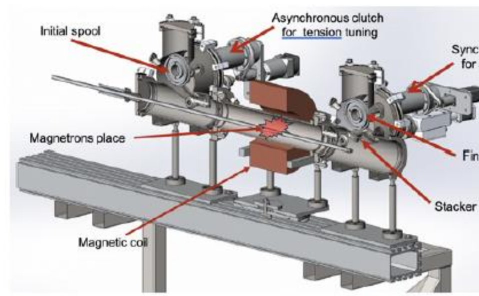

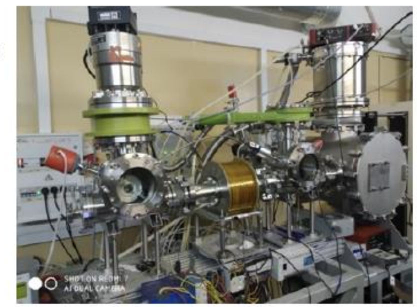

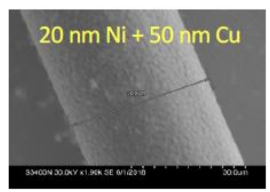

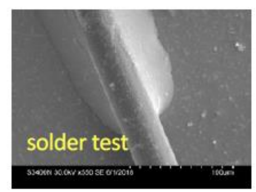

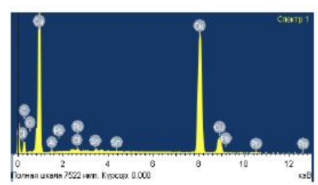

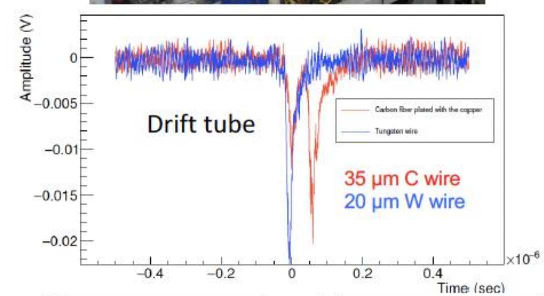

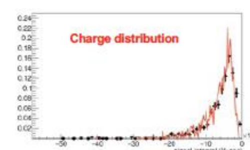

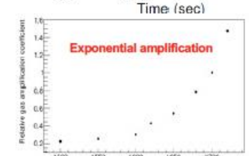

2025 full-length prototype: Model

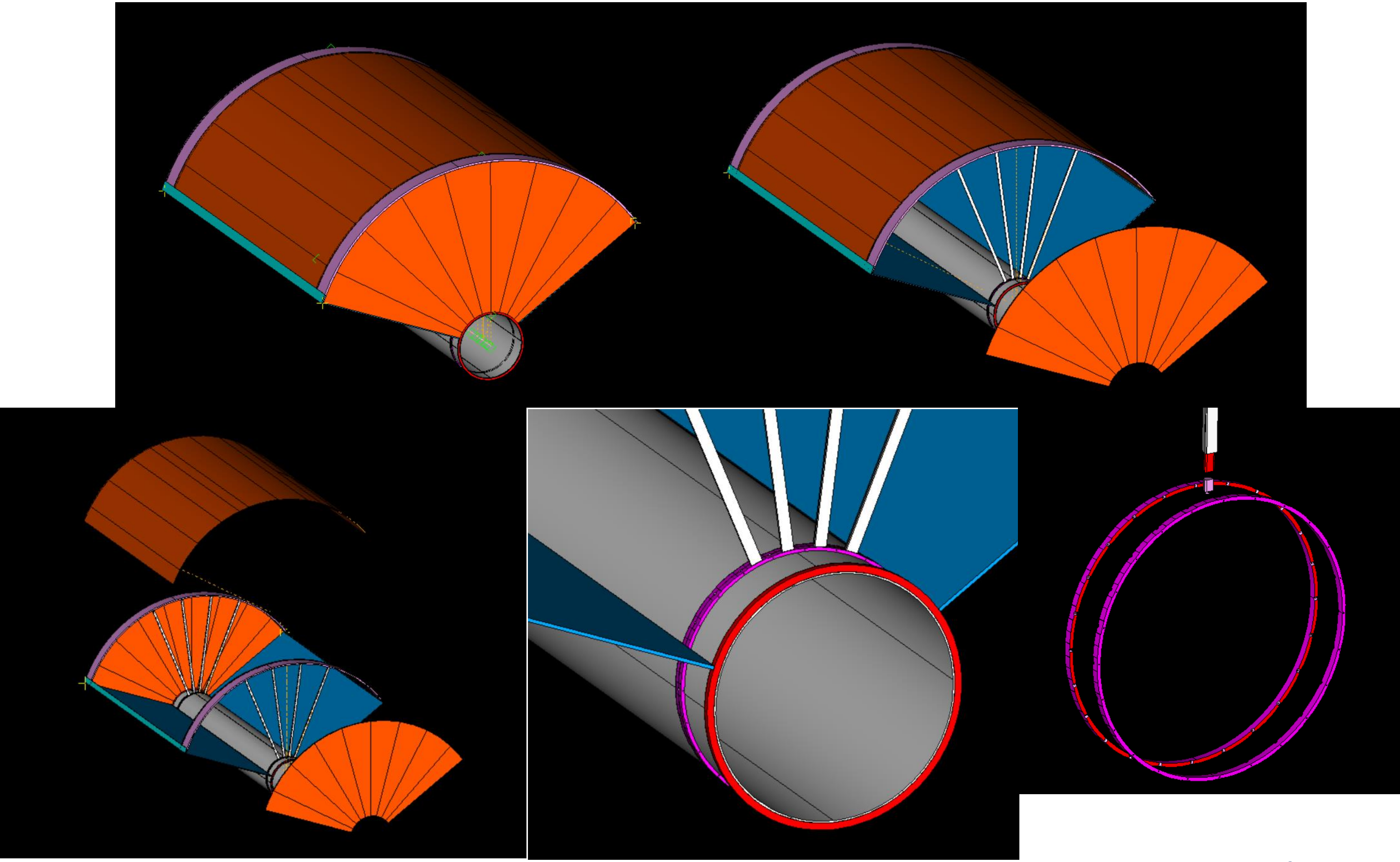

2025 full-length: some arguments

- Three sectors is the minimum for the two stereo views.

- It is necessary to test the innermost layer, with the smallest cells, the outermost layer with the maximum stereo angle and two intermediate layers at the transition of two superlayers, where the pitch of the wires changes for the increase of cells from one superlayer to the next . So, 4 layers for two views, or 8 layers.

- It is necessary to cover the entire sector in azimuth with the wires to distribute the electric field in order to test the electrostatic stability with stereo configurations. Further reducing the number of field wires would involve the introduction of edge effects that would affect the innermost sense wires.

- It is necessary to cover the entire sector in azimuth with wires to control the spinning on PCBs which become approximately 50 cm long at the outermost layer with obvious difficulties in maintaining geometric tolerances.

- Regarding the number of reading channels, we read the two internal views (all 8+8 channels), the four intermediate views (16+16+16+16 channels on 20+20+22+22 sense wires) and the two external views (16+16 channels on 34+34). All this gives a coverage of about 2 dm^2 for vertical cosmic rays.

- The 112 channels → asked support for the two 64-channel NALU cards in addition to the two 16-channel CAEN VX2751 digitizers for comparison and to test the current division reading and the time difference between the two ends of the wires

Full-length prototype: Schedule

- First phase of conceptual design of full chamber completed as of today by a collaboration of EnginSoft and INFN-LE mechanical service (+ a PhD student from Bari Politecnico): final draft of technical report ready
- Full design of full-scale prototype completed by summer 2024 by EnginSoft (purchase order issued) with INFN-LE mechanical service
- Preparation of samples of prototype components (molds and machining) ready by june 2025 by CETMA consortium
- All mechanical parts (wires, wire PCBs, spacers, end plates) ready by june 2026
- MEG2 CDCH2 Wiring robot transported from INFN-PI (being used for MEG2 CDCH2 until May 2024) to INFN-LE/BA, refurbished and re-adapted, to be operational by june 2026
- Wiring and assembling clean rooms:
  - INFN-LE clean room currently occupied by ATLAS ITK assembly (until 2028 ?)
  - Investigating the possibility of renovate a clean room at INFN-BA or at CNR-LE (subject to agreement between INFN and CNR)
- Wiring and assembling operations would occur during second half of 2026
- Prototype built by end of 2027/beginning 2028 and ready to be tested during 2028

N. B. Schedule strongly depending on the funding

2025 full-length prototype: Costs

- Drift Chamber conceptual design (20 k€ from EURIZON-LE, invoice paid to EnginSoft)
- Full-Scale Prototype design (20 k€ from EURIZON-LE, purchase order issued to EnginSoft)
- Full-Scale Prototype design and material tradeoffs (molds and machining) (20 k€ from EURIZON-LE, purchase order issued to CETMA)
- Full-Scale Prototype components (inner cylinder and 8 spokes) (20 k€ from EURIZON-LE, purchase order issued to CETMA)
- Wires from CFW: 10 Km of 50 μm Al for field and guard; 1 Km of 20 μm W for sense (15 k€ from EURIZON-BA)
- Wires from Specialty Materials: 900 m of 35 μm C monofilament (5 k€ from EURIZON-LE)
- Wiring robot from MEG2 CDCH CSN1 funds to INFN-LE (estimated 100 k€)

Costs to be borne (late 2024 and 2025)

- Additional wires
- Wire PCBs
- Peek spacer
- Wiring robot refurbishing
- Mechanical support and gas envelope
- Front-end, digitizers and acquisition electronics

2021/2022 beam test results: gas gain scan

The range of gas gain, independently of the drift tube configuration (drift length, sense wire diameter, gas mixture), lies within 1×10⁵ and 5×10⁵.

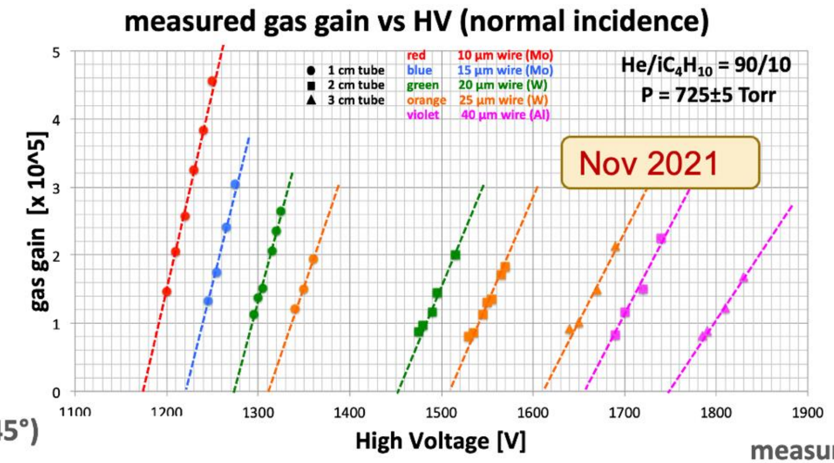

20µm wire excluded from physical quantities mean computation

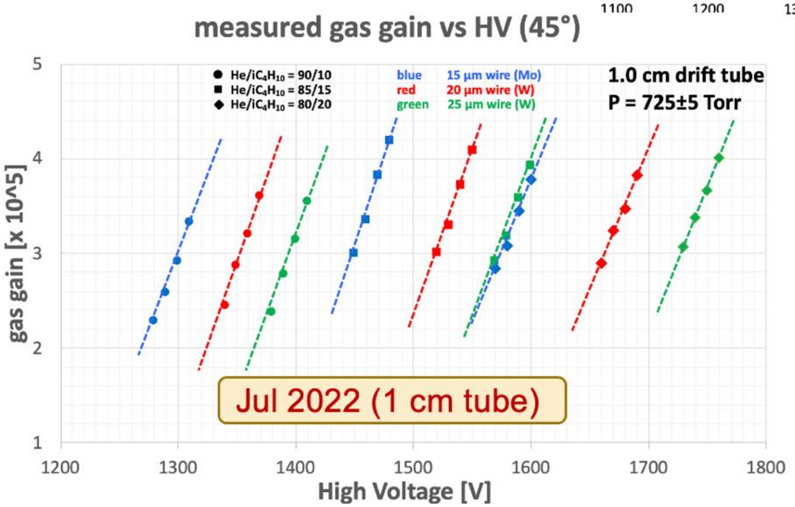

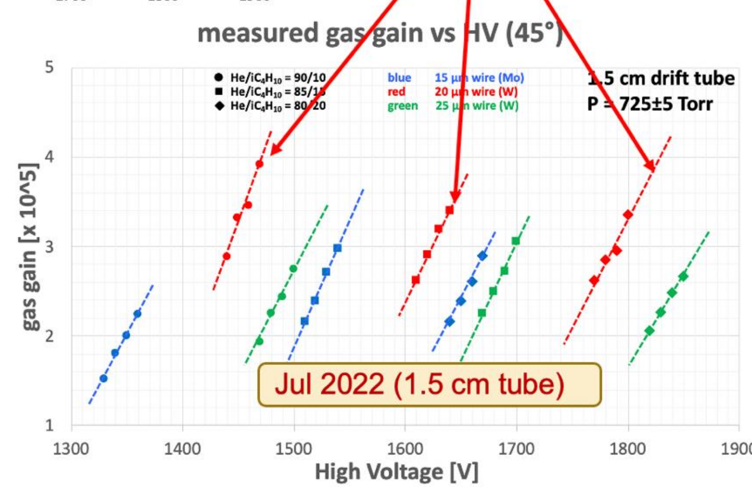

The Drift Chamber: Cluster Counting/Timing and PID

- Analitic calculations: Expected excellent K/π separation over the entire range except 0.85<p<1.05 GeV (blue lines)

- Simulation with Garfield++ and with the Garfield model ported in GEANT4:
  - the particle separation, both with dE/dx and with dN_{cl}/dx, in GEANT4 found considerably worse than in Garfield
  - the dN_{cl}/dx Fermi plateau with respect to dE/dx is reached at lower values of βγ with a steeper slope
  - finding answers by using real data from beam tests

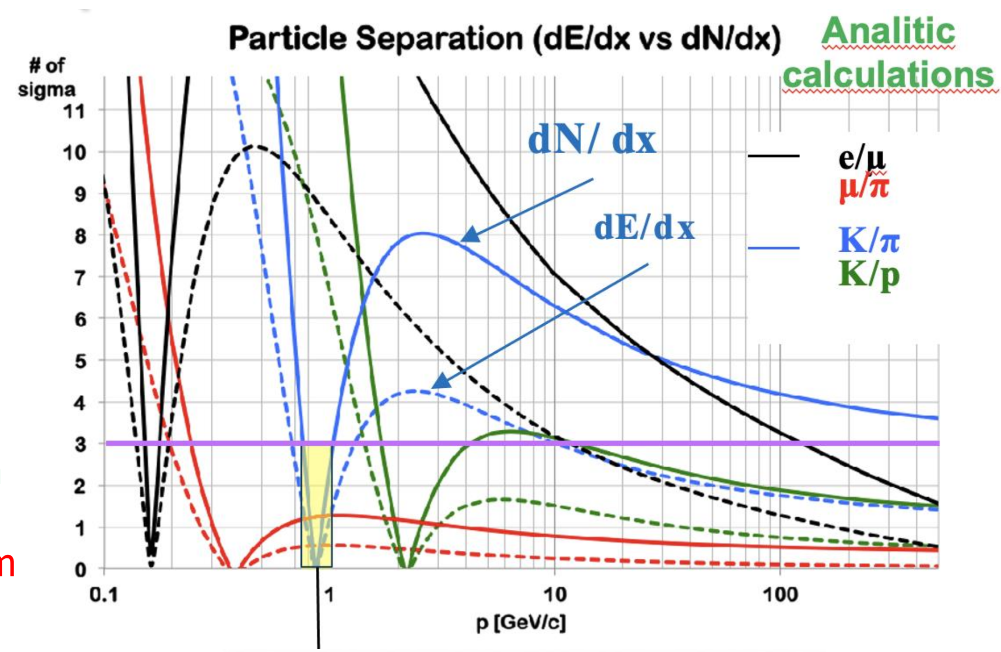

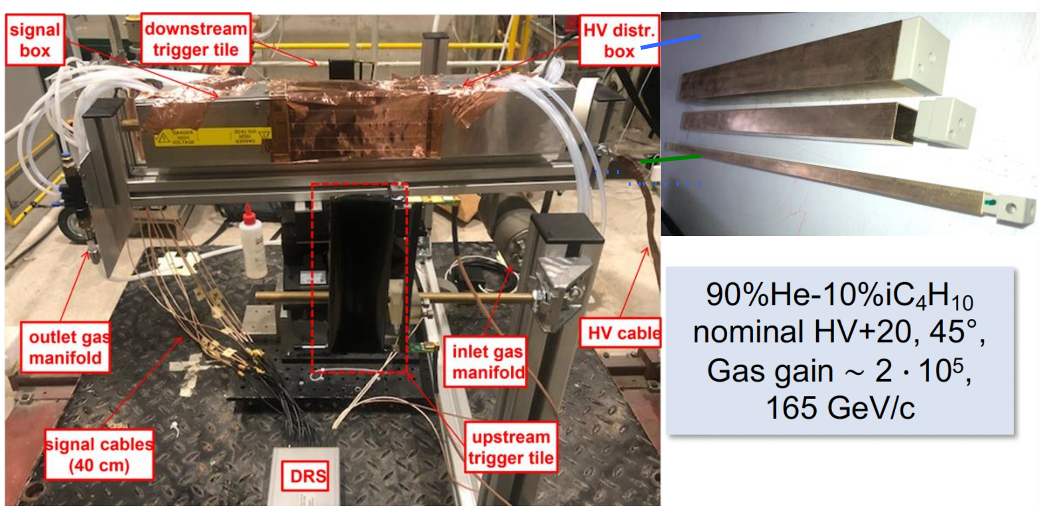

90%He-10%iC_4H_{10}
nominal HV+20, 45°,
Gas gain ~ $2 \cdot 10^5$,
165 GeV/c

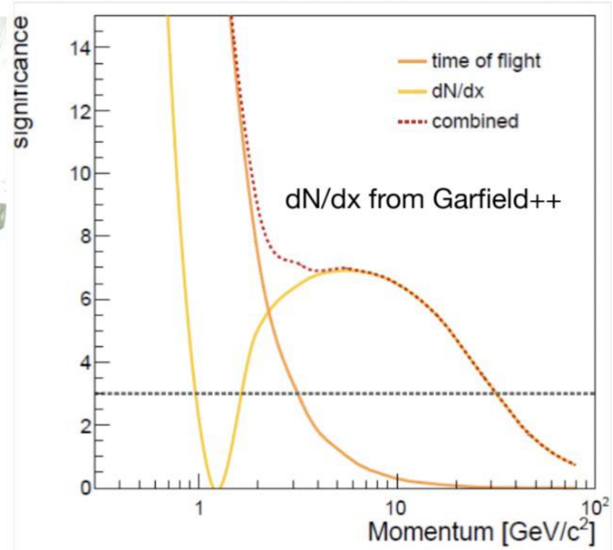

Peak finding algos: Derivative vs RTA

Derivative Algorithm (DERIV)

Find good electron peak candidates at position bin n and amplitude A_n :

- Compute the first and second derivative from the amplitude average over two times the timing resolution and require that, at the peak candidate position, they are less than a r.m.s. signal-related small quantity and they increase (decrease) before (after) the peak candidate position of a r.m.s. signal-related small quantity.
- Require that the amplitude at the peak candidate position is greater than a r.m.s. signal-related small quantity and the amplitude difference among the peak candidate and the previous (next) signal amplitude is greater (less) than a r.m.s. signal-related small quantity.
- NOTE: r.m.s. is a measurements of the noise level in the analog signal from first bins.

Running Template Algorithm (RTA)

- Define an electron pulse template based on experimental data.
- Raising and falling exponential over a fixed number of bins (Ktot).
- Digitize it (A(k)) according to the data sampling rate.
- The algorithm scan the wave form and run over Ktot bins by comparing it to the subtracted and normalized data (build a sort of χ^2).
- Define a cut on χ^2.
- Subtract the found peak to the signal spectrum.
- Iterate the search.
- Stop when no new peak is found.

k	A(k)
0	0.0
1	0.269
2	1.0
3	0.744
4	0.545
5	0.390
6	0.269
7	0.175
8	0.102
9	0.044
10	0.0

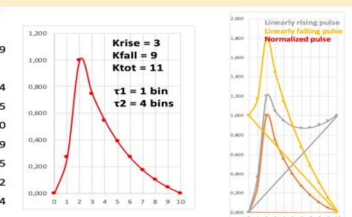

N. De Filippis

Peak finding algos: clusterization algo

Sense Wire Diameter 15 μm; Cell Size 1.0 cm; Track Angle 45; Sampling rate 2 GSa/s; Gas Mixture He:IsoB 80/20

- ***Merging of electron peaks in consecutive bins in a single electron to reduce fake electrons counting.***
- ***Contiguous electrons peaks which are compatible with the electrons' diffusion time (it has a*** $\sim\sqrt{t_{ElectronPeak}}$ ***dependence, different for each gas mixture) must be considered belonging to the same ionization cluster. For them, a counter for electrons per each cluster is incremented.***
- ***Position and amplitude of the clusters corresponds to the position and height of the electron having the maximum amplitude in the cluster.***
- ***Poissonian distribution for the number of clusters!***

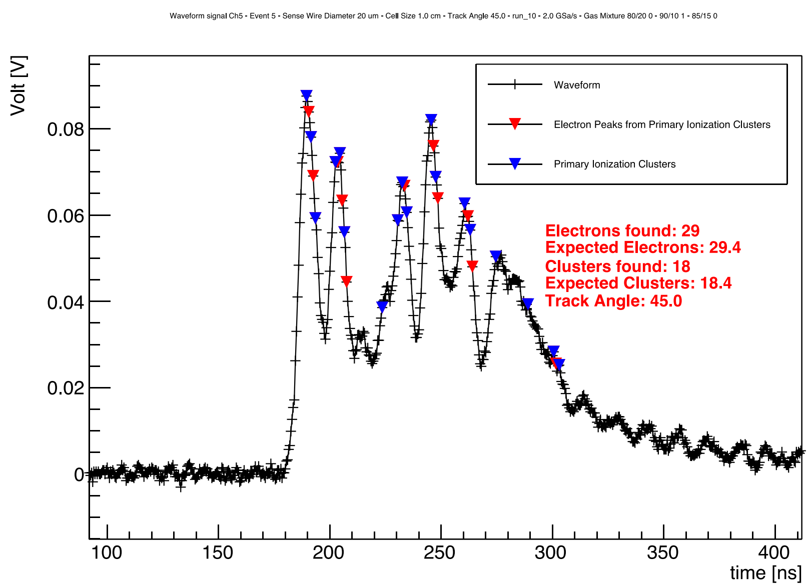

New strategy for digitization for the DCH

M. Saiel, N. De Filippis, G. Tassielli

- Result of a hit cell digitization at the **lowest level, L_0**, must be **a waveform**

- At a higher **level, L_1**, results of hit digitization are:
  - list of electron peak positions and relative amplitudes (i.e., ionization electrons after peak finding –red markers in the picture) or
  - list of ionization cluster positions and relative amplitudes (after electrons clusterization algorithm –blue markers in the picture)

- At an even higher **level, L_2**, results of hit digitization are:
  - impact parameter.
  - number of clusters.

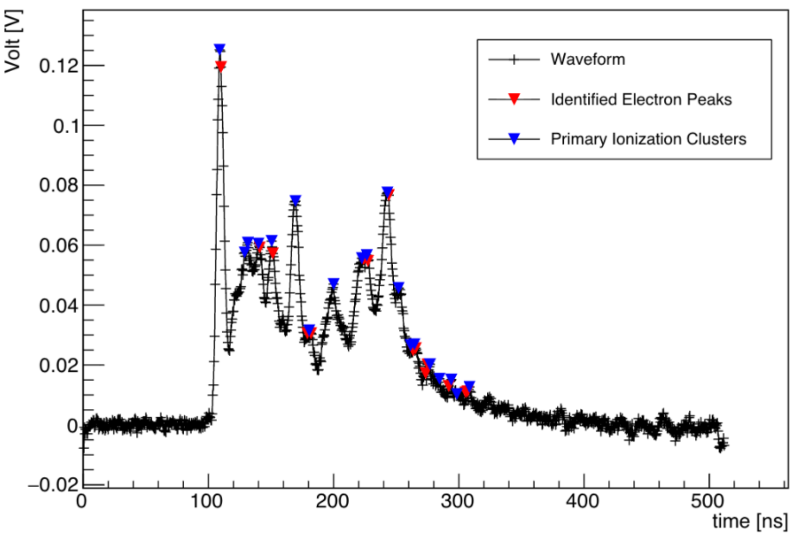

Track finding: performance of the current IDEA

For the Geant4 based simulation framework code:

$$\frac{\Delta p_T}{p_T}\Big|_{res.} = \frac{\sigma_{r\phi}\, p_T}{0.3\, B_0 L_0^2}\sqrt{\frac{720N^3}{(N-1)(N+1)(N+2)(N+3)}} \approx \frac{12\,\sigma_{r\phi}\, p_T}{0.3\, B_0 L_0^2}\sqrt{\frac{5}{N+5}}$$

$$\frac{\Delta p_T}{p_T}\Big|_{m.s.} = \frac{N}{\sqrt{(N+1)(N-1)}}\,\frac{0.0136\,\mathrm{GeV/c}}{0.3\beta\, B_0 L_0}\sqrt{\frac{d_{tot}}{X_0\sin\theta}}\left(1+0.038\ln\frac{d}{X_0\sin\theta}\right)$$

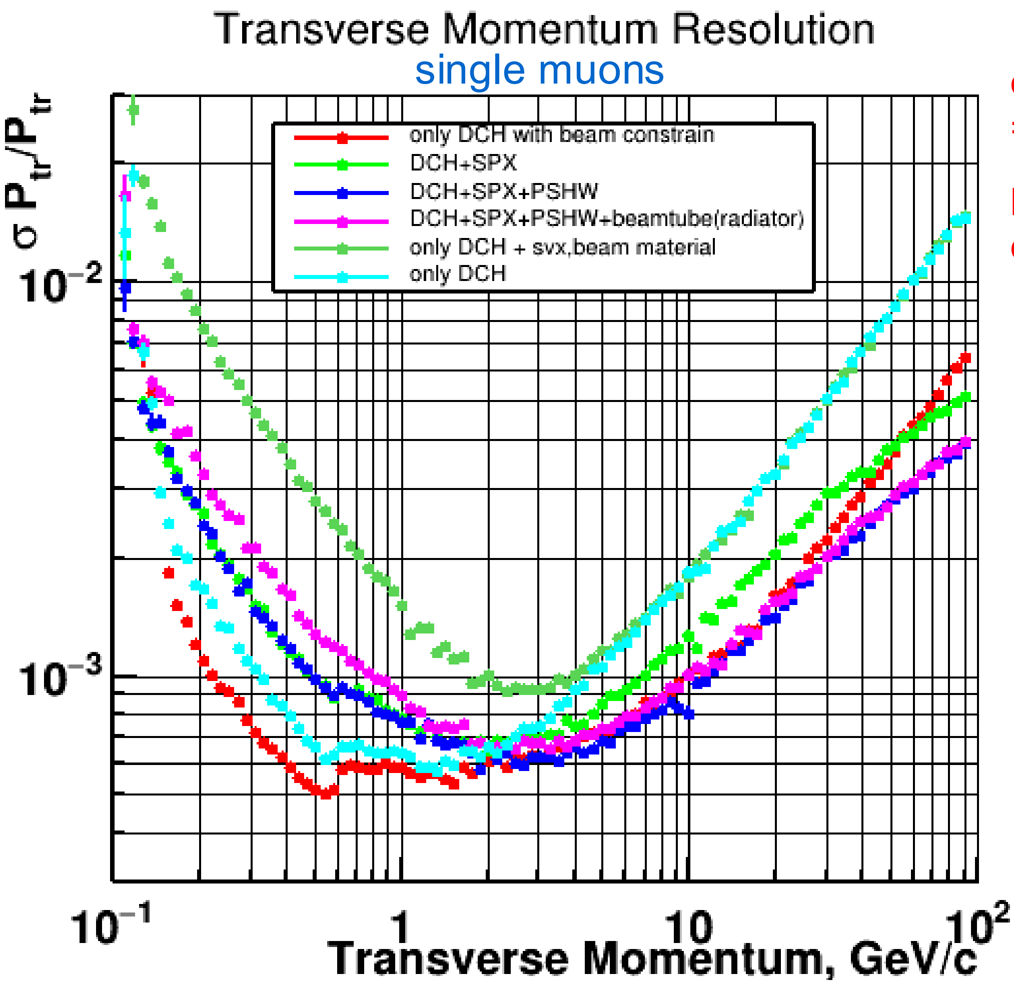

$\sigma(p_t)/p_t$ (100 GeV) $= 3\times10^{-3}$

but new studies ongoing

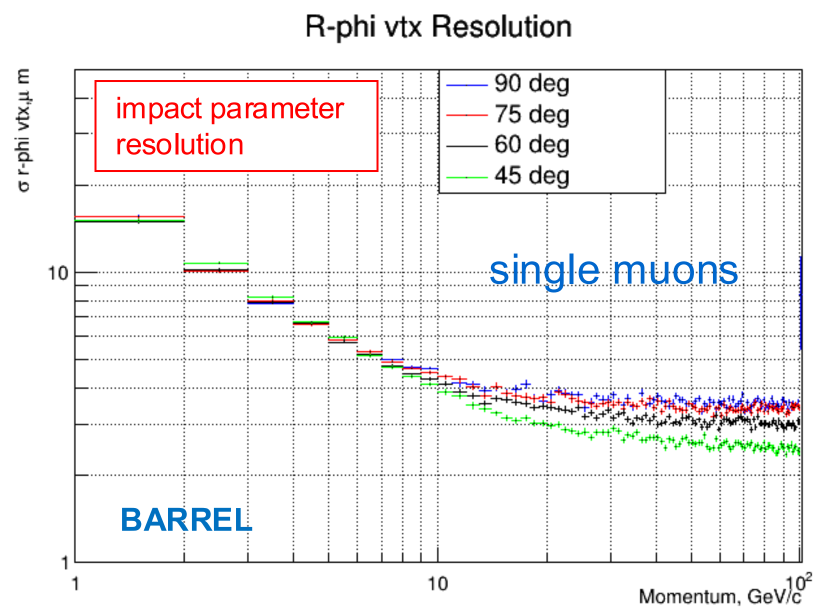

$\sigma(d_0)$ (100 GeV) = 2μm

N. De Filippis

Constraint from Higgs Mass measurement

Higgs boson mass to be measured with a precision better than its natural width (4MeV), in view of a potential run at the Higgs resonance

Higgs mass reconstructed as the recoil mass against the Z, M_{recoil} , and solely from the Z

$$M^2_{recoil} = (\sqrt{s} - E_{l\bar{l}})^2 - p^2_{l\bar{l}} = s - 2E_{l\bar{l}}\sqrt{s} + m^2_{l\bar{l}}$$

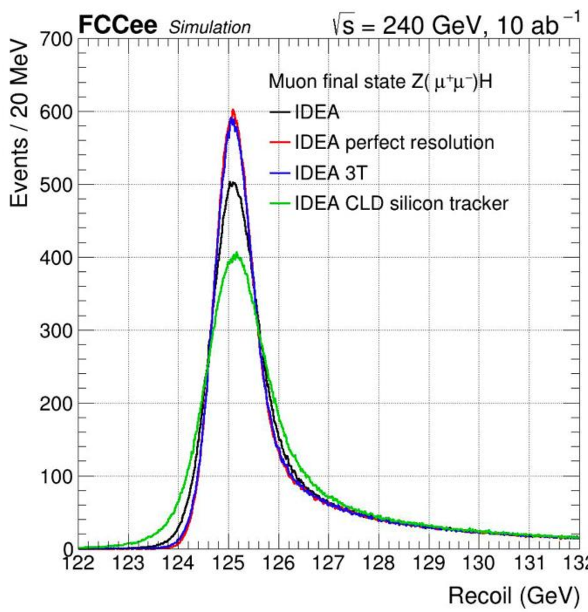

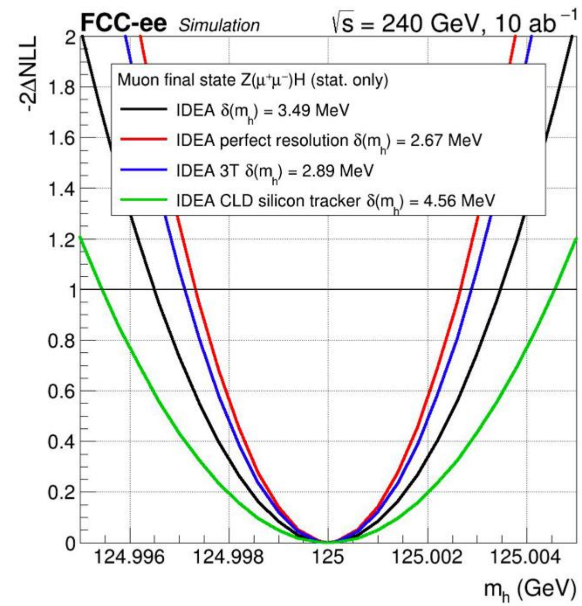

μ from Z, with momentum of O(50) GeV, to be measured with a p_T resolution smaller than the BES in order for the momentum measurement not to limit the mass resolution

- achieved with the baseline IDEA detector → uncertainty of 4.27 MeV with 10 ab^{-1}
- CLD performs less well because of the larger amount of material → larger effects of MS

If the B increased from 2T to 3T → 50% improvement of the momentum resolution
14% improvement on the total mass uncertainty

Challenge: Data reduction and pre-processing

The excellent performance of the **cluster finding** algorithms in offline analysis, relies on the assumption of being able to transfer the full spectrum of the digitized drift signals. However …

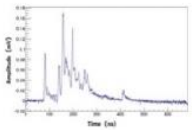

according to the **IDEA drift chamber operating conditions**:

- 56448 drift cells in 112 layers (~130 hits/track)
- maximum drift time of 500 ns
- cluster density of 20 clusters/cm
- signal digitization 12 bits at 2 Gsa/s

… and to the **FCC-ee running conditions at the Z-pole**

- 100 KHz of Z decays with 20 charged tracks/event multiplicity
- 30 KHz of $\gamma\gamma \longrightarrow$ hadrons with10 charged tracks/event multiplicity
- 2.5% occupancy due to beam noise
- 2.5% occupancy due to hits with isolated peaks

Reading both ends of the wires, ⇨ data rate ≥ 1 TB/s !

Solution consists in transferring, for each hit drift cell, instead of the full signal spectrum, only the minimal information relevant to the application of the **cluster timing/counting techniques**, i.e.:

the amplitude and **the arrival time** of each peak associated with each individual ionisation electron.

This can be accomplished by using a **FPGA** for the **real time analysis** of the data generated by the drift chamber and successively digitized by an ADC.

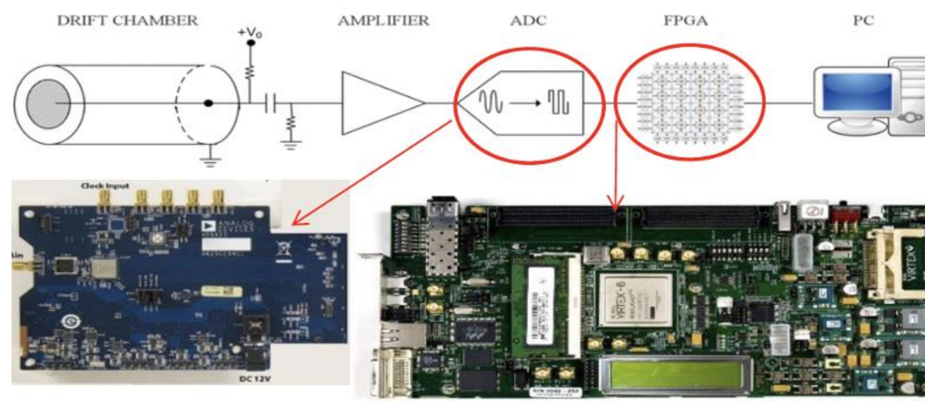

Single channel solution has been successfully verified.

G. Chiarello et al., The Use of FPGA in Drift Chambers for High Energy Physics Experiments May 31, 2017
DOI: 10.5772/66853

With this procedure **data transfer rate is reduced to ~ 25 GB/s**
Extension to a 4-channel board is in progress. Ultimate goal is a multi-ch. board (128 or 256 channels) to **reduce cost** and complexity of the system and to gain flexibility in determining the **proximity correlations** between hit cells for track **segment finding** and for **triggering** purposes.

Implementing ML algorithms on FPGA for peak finding

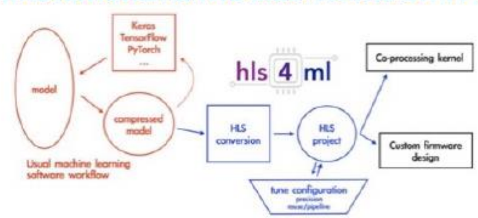

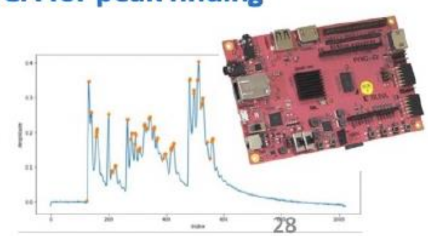

N. De Filippis